JOURNAL OF MATERIALS SCIENCE 27 (1992) 6533–6563

Review
Various aspects involved in the production of low-hydrogen aluminium castings

A. M. SAMUEL, F. H. SAMUEL
Department of Applied Sciences, Université du Québec à Chicoutimi, Chicoutimi, Québec, Canada G7H 2B1

The various areas involved in the casting process of aluminium alloys are all interrelated with each other and revolve around one primary concern: the hydrogen content present in the molten alloy prior to and during casting and its consequential effect on the porosity and quality of the cast product. Focusing on this concern, the present article reviews the problems associated with the production of aluminium alloy castings, in particular those areas on which the hydrogen content has a direct bearing. Current procedures in each area are discussed.

1. Introduction

With the increasing trend in the use of aluminium foundry alloys for the production of critically stressed components in the automotive and aerospace industries, the aluminium industry has had to focus sharply on the quality and reliability of such component castings.

The consequent need for a thorough comprehension of all factors that can possibly affect the structural integrity of such castings is amply reflected in the mass of literature that is available today, covering various aspects of casting in relation to aluminium.

To consistently produce high-quality castings, the alloy or metal quality must be optimized prior to casting. This is achieved by paying attention to important aspects of the processing like melt composition, modification, degassing, inclusion removal, grain refinement and heat treatment.

Considering the other side of the coin, namely that of defects, porosity in a casting can be regarded as one of the major factors critical to its quality. The presence of porosity, inevitable to a certain extent in any casting, can be very detrimental, not only in terms of surface quality after machining, but also, more importantly, in terms of its effect on the mechanical properties and corrosion resistance.

Porosity in castings occurs because of the rejection of gas from solution during solidification and/or the inability of the liquid metal to feed through the interdendritic regions to compensate for the volume shrinkage associated with the solidification. Hydrogen is the only gas capable of dissolving to a significant extent in molten aluminium. The dramatic decrease in its solubility at the solidification point of aluminium, resulting in outgassing, leads to the formation of porosity and reduced mechanical properties and corrosion resistance. Many researchers have reported results showing the deleterious effect of gas content. Thus the control of dissolved hydrogen levels in molten aluminium alloys is a critical parameter for quality control requirements in castings, particularly where high-strength alloys are concerned.

This brings one to the realm of degassing. Several methods are currently in use to degas aluminium. The use of nitrogen or argon as a purge gas is the most common, followed by that of commercially available nitrate or carbonate tablets that release hexachloroethane when plunged into the melt. The degassing process is backed by mathematical models that show the dependence of the process on the metal temperature and the nature of the purge gas. More recent trends are inclined towards the use of flux injection, rotary impellor as well as vacuum degassing techniques.

Besides hydrogen concentration, the formation of porosity is also controlled by other factors like grain refining and inclusion content. Grain refiners are added in small amounts to molten aluminium alloys to control the grain structure in the casting. Al–Ti and Al–Ti–B master alloys are usually employed, where $TiAl_3$ particles act as nucleating sites for the formation of primary α-aluminium dendrites and promote a uniform, equiaxed grained structure, leading to a finer dispersion of porosity and, in some cases, a reduction in the amount of porosity.

Grain refiners are, however, only one among the several non-metallic inclusions that can be present in a melt, others including refractory materials, furnace oxides, dross, etc. These inclusions can be typically 1 to 30 μm in size, liquid- or solid-type in nature, and their presence can lead to several problems, including increased porosity, poor surface quality and machinability, with drastic reductions in the mechanical properties.

Filtration is the most common technique of inclusion removal. Various materials have been used

0022–2461

as filters so far in foundries, including wire wool, steel gauze screens, fibre glass cloths and more recently, ceramic foam filters. The filtration process can be deep bed or cake type. The filtration system for the ceramic foam filters is different from either of these, however.

The complex phenomenon of inclusion removal is as yet not well understood, in spite of the tremendous amount of effort expended to eliminate inclusions. There is an urgent need for the development of simple, accurate and inexpensive techniques to measure inclusion content; a lack in this respect has left the aluminium foundry wanting in a complete understanding of inclusion removal and its related problems.

Modification is yet another area of considerable importance, albeit somewhat controversial, in aluminium casting. In Al–Si hypoeutectic alloys, it involves the addition of an element such as Na or Sr to the melt in order to change the shape of the eutectic Si from acicular to fibrous. The modified eutectic structure results in improved mechanical properties of the casting. However, this advantage is offset by the fact that, due to the resulting enhancement of the susceptibility of these alloys to hydrogen absorption (commonly referred to as "hydrogen pick-up"), modified castings generally exhibit an increased amount of porosity when compared to unmodified ones. This is significant in that the increased porosity can adversely affect the mechanical properties.

Many investigations have been carried out to assess the microstructural characteristics of Al–Si and other Al alloys and to determine the extent of the benefits of modification.

With respect to Na and Sr in particular, it has been found that the microstructural and property changes caused by strontium modification are comparable to those obtained with sodium. Both elements lead to a depression of the eutectic temperature, a modification in the eutectic silicon morphology from plates to fibres, and an increase in the primary aluminium solid solution phase. However, there also exist obvious differences between the two modifiers.

Until a few years ago, there was a general lack of experimental data to substantiate the differences reported in the behaviours of Na and Sr. The matter is still not resolved and the present situation shows that there are two schools of thought prevalent in this area: one that believes that Sr is slightly, if at all, a better modifier than Na; the other upholds the superiority of Sr over Na by virtue of various experimental observations, the details of which will be discussed later on in this article.

It is interesting to observe how the various areas involved in the casting process are interrelated with each other, all revolving around one primary concern: the hydrogen content present in a molten alloy prior to casting and its consequential effect on the porosity and quality of the cast product. Focusing on this concern, this article aims to review the problems and technologies associated with the production of aluminium alloy castings, in particular those areas on which the hydrogen content has a direct bearing. State-of-the-art procedures in each area are discussed and commented upon.

2. Hydrogen dissolution

Metallic castings in industry are generally produced in environments where hydrogen is invariably present in the form of water vapour, obtained in large quantities from the combustion products of the fuels used in the furnace, or from moisture in the air or that absorbed on the surfaces of the charge components that are involved during the casting process [1].

Hydrogen is the only gas capable of dissolving to a significant extent in molten aluminium. Upon exposure to the molten metal, the water vapour dissociates to give hydrogen that dissolves as atoms into the melt and oxygen in the form of dross:

$$2Al + 3H_2O \rightarrow Al_2O_3 + 6H$$

The reaction rate increases rapidly with temperature and is even more rapid when Mg is present [2].

Due to the drastic reduction in the solubility of hydrogen at the solidification point of aluminium, there is a lot of outgassing, leading to the formation of porosity and blisters that are detrimental to the properties of the cast product. Thus the control of dissolved hydrogen levels in molten Al alloys is critical to the quality-control requirements for such castings.

Before proceeding to describe the techniques for the analysis and control of hydrogen levels in the alloys, we shall review the theoretical framework essential for the comprehension and proper interpretation of experimental observations.

2.1. Solubility

Hydrogen solubility in metals has been studied by several workers [3–12]. Size factor considerations show that the dissociation must follow the equation

$$H_2(\text{gas}) \rightarrow 2H \text{ (solution)} \qquad (1)$$

where the solubility is represented by the equilibrium constant K for such a reaction. Applying Henry's law (for dilute solutions) and assuming ideal gas conditions, equilibrium is given by

$$K = \frac{a_H^2}{A_{H_2}} \approx \frac{N^2 p^\theta}{p} \qquad (2)$$

where a_H = activity of the solute referred to the atomic fraction at infinite dilution as the standard state, A_{H_2} = activity of the gas referred to the pure gas at a pressure p^θ as the standard state, and N = atomic fraction of solute in equilibrium with an arbitrary gas pressure p.

Expressing Equation 2 in terms of solute concentration and pressure in the gas phase, one obtains the well-known Sieverts' law:

$$\frac{N}{N^\theta} = \left(\frac{p}{p^\theta}\right)^{1/2} \qquad (3)$$

where N^θ is the atomic fraction of solute in equilibrium with the standard pressure p^θ. (N^θ is assumed to possess a value permitted by Henry's law).

From Equations 2 and 3 one can express the variation of solute concentration with temperature (at constant pressure) as

$$\frac{\partial}{\partial T}(\ln K)_P = 2\frac{\partial}{\partial T}(\ln N)_P = \frac{\Delta H^\theta}{RT^2} \quad (4)$$

Considering the standard enthalpy of solution (ΔH^θ) to be constant for a limited temperature range, Equation 4 yields

$$\ln N = -\frac{\Delta H^\theta}{2RT} + \text{constant} \quad (5)$$

It is to be noted, however, that the solubility or the equilibrium concentration of dissolved hydrogen is normally expressed in cm^3 of hydrogen per 100 g of metal, measured at one atmosphere pressure and 273 K. K is therefore expressed in terms of C/C^θ, or C/C_{unit} more appropriately, where C_{unit} represents the standard unit of 1 cm^3 of hydrogen measured at 1 atm and 273 K per 100 g of metal.

Accordingly, Equations 3 and 5 are rephrased as

$$\left(\frac{C}{C_\theta}\right) = \left(\frac{p}{p^\theta}\right)^{1/2} \quad (3a)$$

$$\log\left(\frac{C}{C_{unit}}\right) = -\frac{\Delta H^\theta}{2RT} + \text{constant} \quad (5a)$$

Experimentally obtained values are fitted to this equation and the solubility expressed accordingly.

2.2. Solubility of hydrogen in aluminium and aluminium alloys

Fig. 1a shows the general type of curve obtained for the solubility of hydrogen in aluminium and Al alloys, as reported by different workers. According to Talbot [1], smoothing of these curves gives solubilities for the liquid and solid as

$$\log\left(\frac{C}{C_{unit}}\right) = -\frac{2761}{T[\mathrm{K}]} + 2.768$$

and

$$\log\left(\frac{C}{C_{unit}}\right) = -\frac{2580}{T[\mathrm{K}]} + 1.399$$

respectively. At the melting point of aluminium (660 °C), these values are 0.7 and 0.04 cm^3 per 100 g metal, respectively. As expected, the dissolved concentration shows a linear relation with the square root of the pressure in the gas phase.

Recently, however, after almost three decades, Talbot and Anyalebechi [13] have readdressed the whole situation concerning the solubility of hydrogen in liquid aluminium. According to them, the inconsistencies in the results reported by various workers thus far [4, 6, 7, 10, 14–21] has made the matter of selecting a correct and reliable value for hydrogen solubility in aluminium somewhat difficult to resolve. In the light of this, they have redetermined the value for the temperature and pressure ranges 943–1123 K and 67–113 kPa, respectively, using an appropriate version of Sieverts' method [21]. Based on a critical assessement of their own and others' results, they recommend a value of $(-2700/T) + 2.72$ for the solubility S, when expressed in terms of $\log(S/S_0)$ (S_0 being the same as C_{unit} defined above, and T being the absolute temperature).

They also recommend the use of the Sieverts' method for the determination of the solubility. In their opinion, the merit of Sieverts' method lies in the fact that equilibrium values are measured under equilibrium conditions and it is possible to isolate and evaluate each potential source of error. The sensitivity of the method to these errors is evidenced by the systematic work of Ransley and Neufeld [6] and Opie and Grant [7], whose observations discredited the results of earlier workers [4, 14–20] who had not

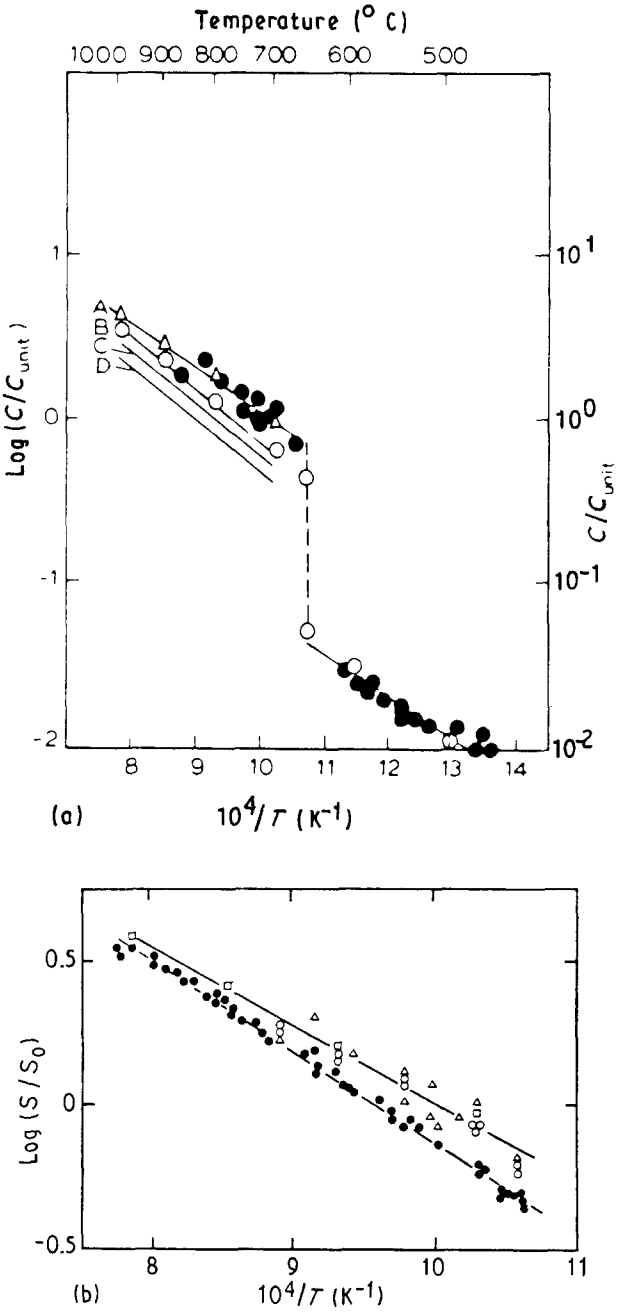

Figure 1 (a) Solubility of hydrogen in aluminium and aluminium alloys [1]. (A) Pure aluminium: (●) Ransley and Neufeld [6], (△) Opie and Grant [7], (○) Eichenauer *et al.* [10]. Alloys: (B) Al–10 Si, (C) Al–8 Cu, (D) Al–16 Cu, all from Opie and Grant [7]. (b) Solubility of hydrogen in liquid aluminium [13]: (○) Talbot and Anyalebechi [13], (△) Ransley and Neufeld [6], (□) Opie and Grant [7], (●) Eichenauer *et al.* [10].

properly evaluated or accounted for these errors in their investigations.

Fig. 1b depicts the solubility of hydrogen in liquid aluminium as obtained by these authors. The results of Ransley and Neufeld [6], Opie and Grant [7] and Talbot and Anyalebechi [13] agree closely and are attributed by the latter as being representative of the Sieverts method used by all three groups. In comparison, the values of Eichenauer *et al.* [10] are much lower, probably on account of the isothermal absorption/desorption method used by them instead, which is prone to systematic error. Further supporting their claim, Talbot and Anyalebechi [13] report that a comparison of hydrogen contents using the Telegas instrument and vacuum hot extraction method [22–24] yields results that are in excellent agreement if solubility values given by these three sets of authors are used but not if those of Eichenauer *et al.* [10] are applied. It may be mentioned in passing that, in a subsequent publiciation [11], Eichenauer has admitted that data given in their first paper were too low.

It is also interesting to note at this point that, with regard to measurements on the diffusivity of hydrogen in aluminium, Talbot in one of his earlier works [1] has emphasized the use of sound material and in this connection recommends the results of Eichenauer and Pebler [25] as being reliable rather than those of Ransley and co-workers [26, 27] who used defect-containing materials (see section 2.4 below on diffusivity).

The 1938 work of Baukloh and Oesterlen [4] is among some of the earlier results reported for the solubility of hydrogen in aluminium alloys. Reporting on the effect of copper and silicon additions, these authors noticed a definite minimum in the solubility at 6 wt % for both copper and silicon, where the solubility of hydrogen was seen to decrease rapidly with the addition of these elements. However, no explanation was given for these minima.

Later on, Opie and Grant [7] undertook to check results reported for the solubility of hydrogen in aluminium as well as study the effects of alloy additions. Using the well-known Sieverts method [21] they determined the solubility of hydrogen in pure aluminium and Al–Si and Al–Cu alloys. According to them, copper and silicon both decreased the solubility of hydrogen in aluminium, the former being more effective than the latter. Contrary to Baukloh and Oesterlen [4], no minimum was noted for the hydrogen solubility versus copper/silicon content. The solubility results determined at various pressures in these alloys showed that Sieverts' law was obeyed.

It is of interest to note that in connection with investigations in 1961 on the effects of Si content and local solidification time on hydrogen content in relation to the formation of porosity in Al–Si alloys, Šarov (reported by Honer and Youling [28]) obtained similar minima at 6 wt % Si as were reported by Baukloh and Oesterlen [4]. Fig. 2a depicts these results.

Recently, Lin and Hoch [29] have calculated the solubility of hydrogen in molten aluminium alloys containing copper, lithium, magnesium and silicon, from the solubility of hydrogen in pure metals and binary metal–metal interaction parameters, applying the thermochemical model developed by Hoch and Arpshofen [30]. According to them, the excellent agreement between their calculated results based on this model and the experimental data of Opie and Grant [7] for the solubility of hydrogen in Al–Cu alloys lends support to the suitability of this model in the prediction of the thermodynamic properties of a ternary solution from the corresponding binary systems. Accordingly, they have evaluated the thermodynamics of the Al–H, Cu–H, Mg–H, Li–H, Al–Cu, Al–Si, Al–Mg, Al–Li, Al–Li–H, Al–Cu–H, Al–Mg–H and Al–Si–H systems. Fig. 2b, c and d depict the solubility of H in molten Al–Cu, Al–Li and Al–Mg alloys, respectively, as reported by Lin and Hoch [29]. Some experimental data points are available for comparison in the Al–Cu and in the Al–Mg case, but none are available for the Al–Li alloys.

2.3. Effect of modification: hydrogen pick-up

Linked to the solubility of hydrogen in aluminium is the way it is affected by modification. Modification has been known to increase the susceptibility of these alloys to hydrogen pick-up [31]. While the advantages of eutectic modification are directly perceived in the improved mechanical properties of such alloys, some caution is, nevertheless, still exercised in its use, since modified castings tend to exhibit an increased porosity. This porosity has been connected to the increase in hydrogen absorption by the melt in the presence of such modifiers [32–35].

Although sodium has long been the traditional modifier, the feasibility of using strontium as an alternative for Al–Si alloys has been receiving increasing attention in the last three decades. With the introduction of Sr-containing master alloys that helped overcome the difficulties previously associated with its use in elemental form, there has been a greater acceptance of Sr as a modifier. Master alloys are now available as Al–Sr (5–10%) or Al–15 Si–10 Sr alloys. A number of studies have been carried out on the solidification of Sr-modified alloys [32–40], including those on the burn-off rate of Sr [36, 41] and optimum levels of Sr addition for modification [42, 43].

The effects of Sr on the microstructure and properties are comparable to those of Na. Among other things, both elements modify the eutectic Si morphology from plates to fibres, refine the eutectic, increase the primary Al solid-solution phase and depress the eutectic temperature. However, Sr possesses a number of advantages over sodium, the main one being that it is a "permanent" or long-term modifier, while Na is easily lost from the melt by volatilization and oxidation [42]. Various studies have been carried out on the modification behaviour of Na and Sr. Differences or similarities have been reported, depending on the individual study [2].

Pertaining to our present discussion, concerning the susceptibility of modified melts to hydrogen absorption, while some investigators report that Sr behaves

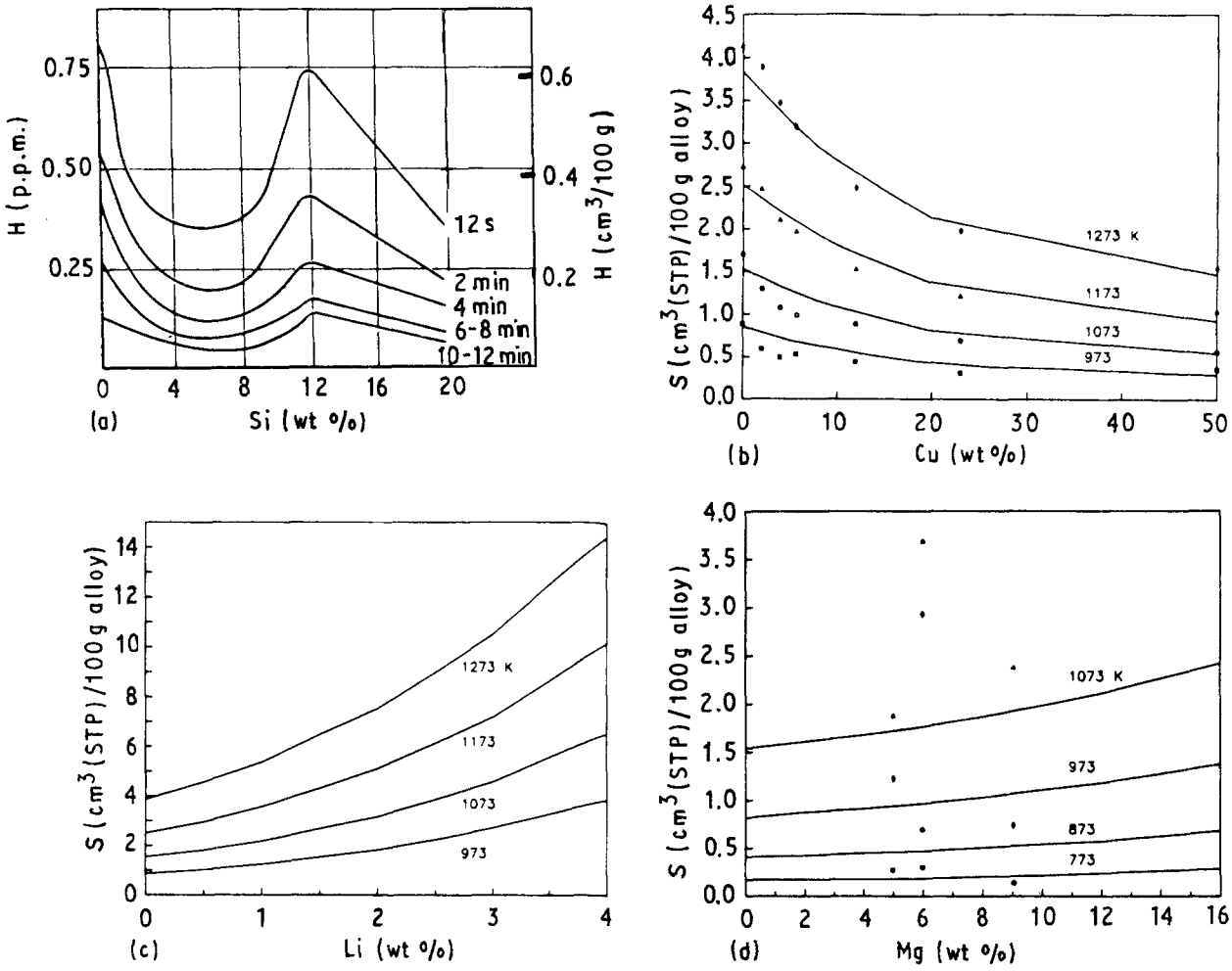

Figure 2 (a) Hydrogen content giving rise to porosity in Al–Si alloys at different solidification times [28]. (b) Solubility of hydrogen in molten Al–Cu alloys (data points from Opie and Grant [7]): (■) 973 K, (●) 1073 K, (▲) 1173 K, (◆) 1273 K, (——) calculated. (c) Solubility of hydrogen in molten Al–Li alloys. (d) Solubility of hydrogen in molten Al–Mg alloys (data points from Baukloh and Oesterlen [4]): (■) 773 K, (●) 873 K, (◆) 973 K, (▲) 1073 K, (——) calculated. Solid lines are the estimated values as reported by Lin and Hoch [29].

similar to Na in increasing gas pick-up [33], others find that Sr is more effective in doing so [28, 31, 32]. In contrast to both, according to Traenkner [2], it is Na that is preferred to Sr in foundries because it generates more gas than Sr. In Gruzleski's opinion [44] there is, apparently, considerable evidence to suggest that higher hydrogen levels are not associated with the use of Sr, and that under certain conditions, Na modification also does not result in more melt-dissolved hydrogen.

Sizing up various reports, Na and Sr possibly have different influences on the pick-up of hydrogen by molten alloys. In fact, the entire question of hydrogen absorption by a molten Al alloy in the presence of a modifier is not well understood and is the subject of conflicting opinions.

In order to clarify some of the pre-existing controversies, Denton and Spittle [31] carried out a detailed investigation of the solidification characteristics of both Sr- and Na- modified Al–Si alloys of the LM6 type, with a view to comparing their susceptibilities to hydrogen pick-up. From their studies, they concluded that Sr increases the susceptibility of Al–Si alloy melts to hydrogen absorption during melting, and that Sr-modified melts are more susceptible to gas pick-up than Na-modified ones.

Another such study was carried out by Dimayuga *et al.* [45] who investigated the degassing and regassing behaviour of Sr-modified A356 Al-alloy melts. They found that Sr modification did not affect the rate of hydrogen pick-up from humid atmospheres by these alloys, and that stirring of the melt significantly increased the rate of hydrogen dissolution. Addition of Sr in the form of 90 Sr–10 Al master alloy did not introduce hydrogen into the melt, i.e. the hydrogen content in the melt remained unchanged. The long-term modifying effect of Sr was also confirmed in their studies. Fig. 3 summarizes the degassing and regassing behaviours of Sr-modified and unmodified melts of A356 alloy as obtained in their work, where the melt was stirred during regassing.

Shahani [46] has investigated the effect of hydrogen content on the shrinkage porosity of Al–Si, Al–Si–Mg and Al–Cu alloys. According to him, the porosity in these castings is dependent on the gas content amongst other factors, and that modifiers (Na, Sr) promote the formation of such type of porosity. In startling contrast to the naturally expected conclusion, however, his results showed that the modified samples had relatively lower hydrogen content, although pores were formed more frequently in such samples.

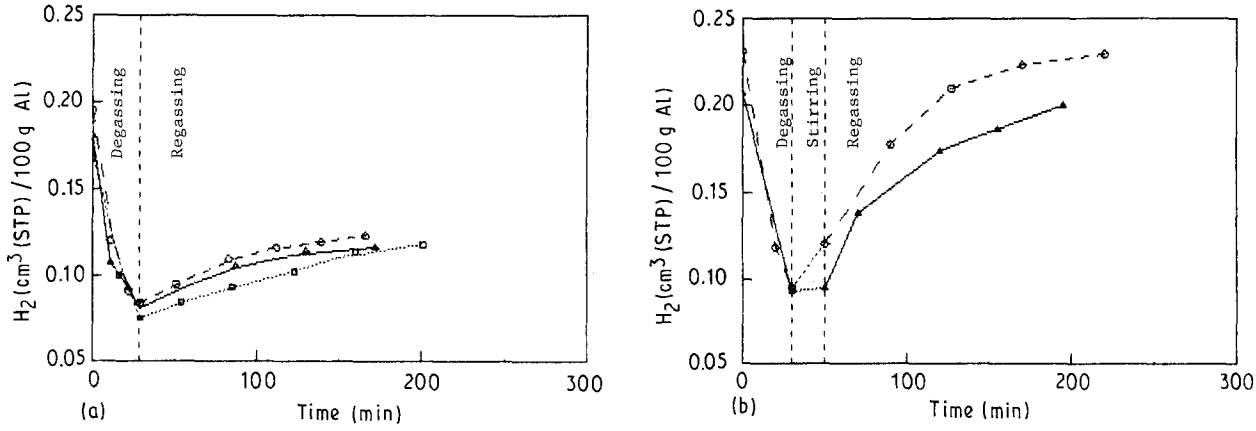

Figure 3 Degassing and regassing behaviour of unmodified and Sr-modified A356 alloy melts (after Dimayuga *et al.* [45]). (a): (△) 0% Sr. (□) 0.014% Sr, (○) 0.021% Sr. (b): (△) without Sr, (○) with Sr.

While studies on modification have mainly centred on Na and Sr, there have been other investigations where the influence of alternative elements has been considered. Honer and Youling [28] have reported on the influence of Ca and Sr on the hydrogen pick-up in Al alloy melts (particularly G-AlSi12 type). Their thermal and microstructural analyses show that Ca acts as a modifying agent, with the severe handicap that even in low concentrations it gives rise to higher hydrogen pick-up and the related danger of porosity. The oxidation of Ca affects the protective oxide skin of the melt and contributes to a faster pick-up of hydrogen by the melt towards equilibrium. According to these authors, even the use of higher concentrations of Sr for long-term modification gives rise to increased sensitivity to hydrogen and thus its content should be carefully decided upon [28] relative to the alloy being modified.

The Bulgarian group of workers Yaneva *et al.* [47] have recently reported on the influence of Sb modification on the hydrogen porosity of Al–Si alloy castings. Their studies reveal that Sb modification allows for the retention of hydrogen in the solid phase, suppressing its tendency to separate as gas in the form of pores during solidification. Thus, despite the increased H content in the alloys, their density remains unchanged, even at low concentrations of the modifier. Thus modification with Sb not only refines the Si phase in Al–Si alloys, but also increases the solubility of the hydrogen in the Al solid solution.

Yet other elements that have been investigated as modifiers include magnesium [48], phosphorus [49] and tungsten [50]. However, these studies are mainly structure–porosity–property oriented, and will not be discussed in the present context. Work on the effect of Sb on Sr-modified A356 melts is likewise discussed in section 4.3 below in connection with porosity.

Summing up, in view of the increasingly widespread use of modifiers in Al–Si castings today, it is essential that the industry should have, first and foremost, a well-defined and consistent picture of how the presence of modifiers affects the rate of hydrogen pick-up and the degassing behaviour of such alloys. In spite of the abounding literature, one can assess that updating in this area is still required.

2.4. Diffusivity

A solute of non-interacting atoms in a single phase diffuses according to Fick's law:

$$\frac{\partial C}{\partial t} = \text{div}(D \text{grad } C) \tag{6}$$

where C and D are, respectively, the concentration and diffusion coefficient of the solute, and t is the time.

In the case of hydrogen, from valency, size and geometrical considerations it is reasonable to assume that the solute must be in the form of non-interacting atoms and occupy equivalent interstitial sites. The diffusion process is thus described by the above equation, standard solutions to which are obtained by considering the initial and boundary conditions, as well as the geometry of the system.

As a rule, diffusion coefficients vary with temperature as

$$D = D_0 \exp\left(-\frac{\Delta G}{RT}\right) \tag{7}$$

where ΔG is the activation energy for diffusion, T is the absolute temperature and D_0 is a constant for the particular system. As can be seen, the variation is Arrhenius-type in nature.

Several workers have reported on the diffusivity of hydrogen in pure aluminium [25–27, 51]. Smithells [52] has compiled an extensive collection of available values for the solubility and diffusivity of hydrogen in metals. For the temperature range 470–590 °C (below the melting point, 660 °C), Eichenauer and Pebler [25] have reported a diffusion coefficient of $0.21 \exp(-45\,600/RT)$ cm^2 s^{-1} for hydrogen in pure solid aluminium. This gives an extrapolated value of 6.0×10^{-4} cm^2 s^{-1} at 660 °C and an expected room temperature value of the order of 10^{-9} cm^2 s^{-1}.

Eichenauer and Markopoulos [51] report a value of $(3.8 \times 10^{-2}) \exp(-4600/RT)$ for the diffusion coefficient in liquid aluminium in the temperature range 780–1000 °C. Their findings show that at the melting point, the rate of diffusion jumps by a factor of six for the liquid state.

Talbot [1] has emphasized the importance of employing sound material in the determination of experi-

mentally obtained coefficients. According to him, the results given by the above authors are reliable, rather than those quoted by others [26, 27] who have reported the presence of defects in their materials.

While Equations 6 and 7 may describe hydrogen solution in liquid metals, the same cannot be applied for solid metals, as this would demand the existence of a structurally perfect material which is not at all the case observed in industrially produced metals. A failure of the regular equations to frequently describe observed behaviour in such materials leads one to believe that the hydrogen within the material is heterogeneously distributed, divided between interstitial solution and hydrogen "trap sites" or lattice defects that trap the hydrogen atoms or molecules. Quenched-in lattice vacancies have been indicated as the defects in question [53].

There is evidence in the literature for atomic traps due to association of interstitial solutes with lattice defects. This is feasible on the basis of the negative binding enthalpy between the solute atoms and the defects due to lattice strain relief. In the case of hydrogen, it has been shown indirectly [54] that the solute segregates to lattice defects.

While the concept of hydrogen trapping receives support from reports of hydrogen diffusion in steel [55–61], the exact nature of these traps has never been elaborated upon [56, 58, 60, 61]. In this respect, it is very interesting to note the comments made by Ishikawa and McLellan [62] in their recent work on the measurement of hydrogen diffusivity in aluminium in the low temperature range 285–328 K. These authors, who have made a detailed comparison and analysis of diffusion data obtained by various workers and by them, negate the notion of the hydrogen-vacancy trapping observable in diffusion measurements at high temperatures. Instead, they purport that, from the agreement between the majority of D values reported at high temperatures and the high-temperature extrapolation of their own data, their results indicate that hydrogen diffusion in solid aluminium occurs by a classical single-mechanism process from 300 K up to the melting point.

Apart from these physical traps, impurities or alloying elements in a metal may react with hydrogen to form precipitates, usually hydrides; the additional hydrogen thus absorbed by the metals is considered to be "chemically" trapped. In the case of aluminium and aluminium alloys, the presence of sodium can lead to such an effect through the formation of sodium hydride [63]. Reactions are typically of the type

$$0.5\,H_2(\text{gas}) + M(\text{in alloy}) \rightarrow MH(\text{ppt})$$

where M is the hydride-forming element, and depend on the activity of the metal in the alloy and the critical hydrogen pressure at which the hydride starts to form.

From the above, it is clear that measurements of solubility and diffusivity of hydrogen in metals are significant only if they have been performed extremely carefully and on materials that are of a sound nature, or at least those whose preparation conditions are well known. Also, the values obtained must be correctly applied to the industrially produced materials. In the case of metals containing hydride-forming elements or very defective materials, there may occur cases when the hydrogen in trap sites could exceed that in solution, impeding the diffusion process [63, 64]. Several mathematical models have been proposed [56, 59, 65] to take into account the effect of traps in steels and these could well be applied to metals. For aluminium, Talbot and Granger [66] have suggested the alternative of applying empirically determined apparent diffusion coefficients directly to industrially produced metals even though they differ from the true coefficients. One must appreciate, none the less, the necessity for a correct estimation of the mobility of hydrogen for practical purposes, as the extent of damaging effects is related to how rapidly the gas can accumulate at critical points (defects) in a metal.

3. Methods of hydrogen measurement

The necessity for an accurate estimation and control of the actual gas level in a metal or alloy prior to and during the melting/casting process at the foundry shop floor level has long been recognized. Due to the sharp decrease in the solubility of hydrogen in aluminium on solidification, even low gas contents can lead to degradation in the properties of the alloy through the formation of gas porosity. As a result, many techniques have been developed, each geared towards greater improvement in the ease of measurement and its accuracy, to meet the needs of the tighter standards imposed today by industry. These techniques range from qualitative, semi-quantitative to quantitative, and can be classified as "direct" or "indirect", depending on whether the actual hydrogen content is measured or whether the observation of some physical characteristic is involved.

Among the earliest tests known for evaluating the hydrogen content in molten aluminium alloys is the Straube–Pfeiffer (S–P) test [67], where the gas content is estimated from the density of a metal sample solidified under reduced pressure. A variation of the test, the "initial bubble test", consists in noting the pressure at which the first bubble is observed in the molten sample kept in a chamber in which the pressure is slowly reduced [68]. The lower the pressure at which the first bubble is noted, the lower the hydrogen content. The Hydro tester produced by Alcan and the Alusuisse/FMA Alu–Melt Tester [69] are based on variations of this approach.

These early tests, however, are not direct measurements of the hydrogen content, being influenced by both hydrogen and inclusion content of the sample. They are more useful as measurements of "metal quality", in which capacity they have actually been used.

The need to measure hydrogen content separately led to the evolution of other techniques of a more absolute nature. Ransley and Talbot [26] were the first to develop a quantitative laboratory analysis technique, variously termed as the "hot extraction", "Ransley's" or "Vacuum subfusion" (VSF) technique. A sample taken from the melt/product is subjected to

careful preparation and heated to a sub-solidus temperature in a good vacuum. The volume of hydrogen gas so extracted is then measured. Although the method has found successful application in the wrought alloy industry, it has not been found suitable for daily use in the foundry.

Focusing their attention on the drawbacks of the VSF technique, and the need to develop an instrument capable of delivering quick hydrogen content determinations, Ransley and co-workers finally developed the Telegas technique in 1957–58, also known as the "closed-loop recirculation" (CLR) technique, to measure the partial pressure of hydrogen in molten aluminium [22, 70].

The underlying principle of the Telegas technique is to create a circulating gas volume within the molten metal, into which hydrogen can diffuse. An inert gas like nitrogen is bubbled through the melt and collected by an inverted bell-shaped probe. After a reasonable time, the dissolved hydrogen in the melt attains an equilibrium with the hydrogen gas contained within the nitrogen bubbles according to

$$2H \rightarrow H_2$$

The concentration of hydrogen in solution in molten aluminium alloys is a function of its solubility and partial pressure and is given by

$$G = kS_0\left(\frac{P_i}{760}\right)^{1/2} \quad (8)$$

where P_i is the equilibrium internal pressure of hydrogen in mm Hg, S_0 is the solubility at 760 mm Hg at a given temperature and k is a constant dependent on the alloy.

The Telegas instrument is designed to measure P_i. The thermal conductivity of hydrogen is greater than that of nitrogen by an order or two of magnitude. Thus the thermal conductivity of the circulating gas is a strong function of the hydrogen concentration, and if the hydrogen content of the nitrogen carrier gas can be measured, this can be directly related to the dissolved hydrogen level in the melt. In the Telegas instrument, this is accomplished with the use of the catharometer (a hot-wire detector) that detects the change in the thermal conductivity, and a Wheatstone bridge circuit. This technique, now marketed by Alcoa (USA), has been found to be adequately precise for quality control work ($\pm$ 0.025 ml per 100 g), and the analysis time is also reasonable ($\sim$ 10 min). A schematic diagram of the Telegas apparatus is shown in Fig. 4a.

In spite of its assets, the original presentation of this technique has quite a few drawbacks. The main drawback concerns the probes, which are expensive, fragile and often break after only a few immersions in the melt, although they are supposedly designed to last through approximately 20–30 analyses. This has been the general experience of various users, as reported in the literature [70, 71]. This results in very high analysis costs. In addition, the Telegas instrument is bulky and the readings can easily be misinterpreted since the instrument only provides arbitrary readings which must be corrected for alloy composition or metal temperature.

Alcoa has now introduced a new compact instrumentation package, Telegas II™, which addresses these problems. It is a completely redesigned instrument that shares only the basic principle with the original Telegas [72]. A self-contained instrument, it displays the gas content directly and can be used anywhere in a plant. Hydrogen partial pressure is measured by a differential thermal conductivity technique. Instead of the original platinum filaments and Wheatstone bridge circuit, a single commerical hot-film sensor is used in a specially developed constant temperature circuit, adapted for gas thermal conductivity changes. Fig. 4b shows a schematic diagram of the Telegas II instrument. The instrument package also incorporates a microprocessor-based control system, a microterminal for operator communication, a printer for hard-based copy output and various memory circuits for storing readings and calibration constants. Although the ceramic probe that is currently utilized is fragile and expensive, it can work well if carefully handled. Other probes with different designs have also been reported and are capable of being used with Telegas II. Alcoa itself is working on several new probe designs that will be less expensive and more durable than the ceramic probe.

As part of an extensive research programme on aluminium alloy melt quality, the quantitative reduced pressure (QRP) and the quantitative recirculating gas (QRG) hydrogen test units have been developed by the BNF Metals Technology Centre. The method of operation is similar to that of Telegas [73].

The other popular alternative to the Telegas technique for hydrogen measurement is the nitrogen carrier fusion (NCF) method. It is a variation of the vacuum subfusion (and, to some extent, the Telegas) method, where the solid sample is heated to above melting point and the hydrogen gas evolved is transported in a carrier gas to be measured by a catharometer or thermal conductivity detector. This technique is available commercially in the form of Leco (RH series) and ITHAC analysers, that are marketed by Leco and Instruments SA, respectively [74].

The Leco RH-3 hydrogen determinator completes an analysis in about 20 min. It operates similarly to the ITHAC-02 analyser, based on the work of Degréve [75, 76]. In these methods, a cylindrical sample placed in a graphite crucible is melted in a stream of nitrogen. The hydrogen is carried downstream to be measured by a catharometer from changes in the thermal conductivity of the carrier gas. The main difference between the two analysers is that the Leco RH-3 is provided with a loading head to introduce the sample into the equipment (see Fig. 4c), making possible the baking out of the crucible and subsequent fusion of the sample without opening the apparatus at any stage of the analysis. With the ITHAC-02, however, it is necessary to open the furnace for sample introduction. Thus, with the Leco RH-3, it is more difficult to introduce atmospheric moisture.

The accuracy of the Leco RH-3 is, in general, satisfactory. However, an appropriate surface-hydrogen

correction has to be applied to the measured values of gas content.

The design of newer, more recent hydrogen analysers are more or less improvements on the Telegas or the NCF methods. Further improvements to the Telegas method have centred on the designing of new probes, to overcome the major drawbacks of the ceramic probe in terms of durability, cost and effectiveness. One of the most recent probes fashioned along these lines is the Alcan probe designed for the AlSCAN analyser, a product of Alcan International and Bomen Inc. of Québec, Canada. This is a new and

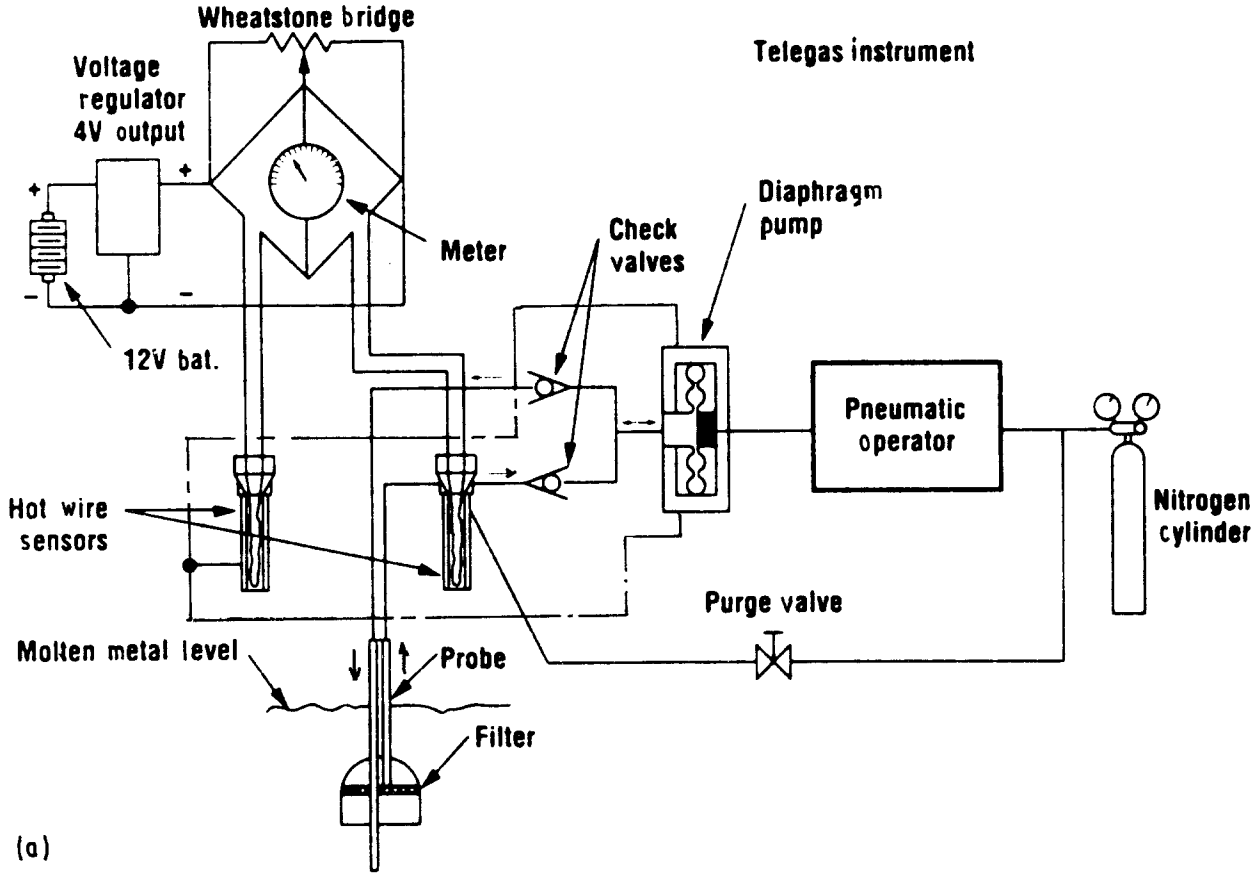

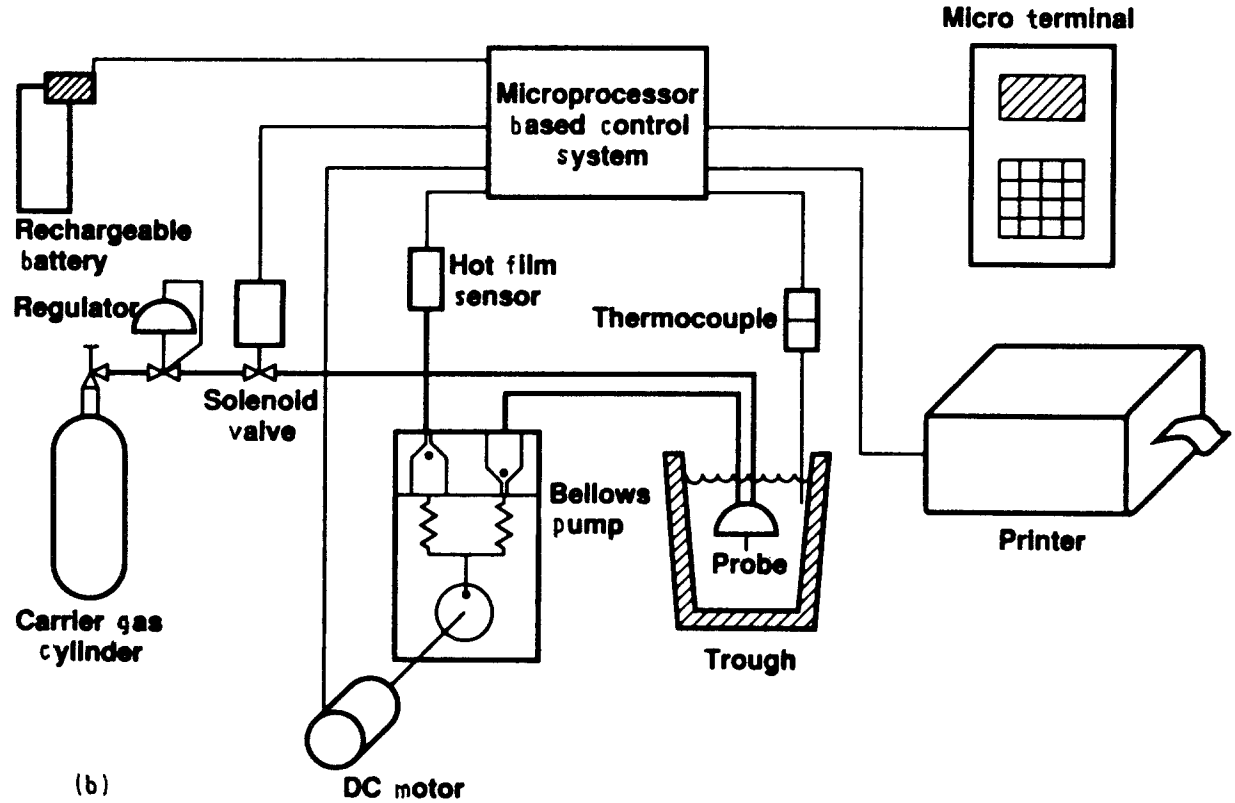

Figure 4 Schematic diagrams of (a) Telegas apparatus [68], (b) Telegas II instrument [73], (c) Leco RH-3 (NCF method) analyser [74], (d) AlSCAN analyser [71].

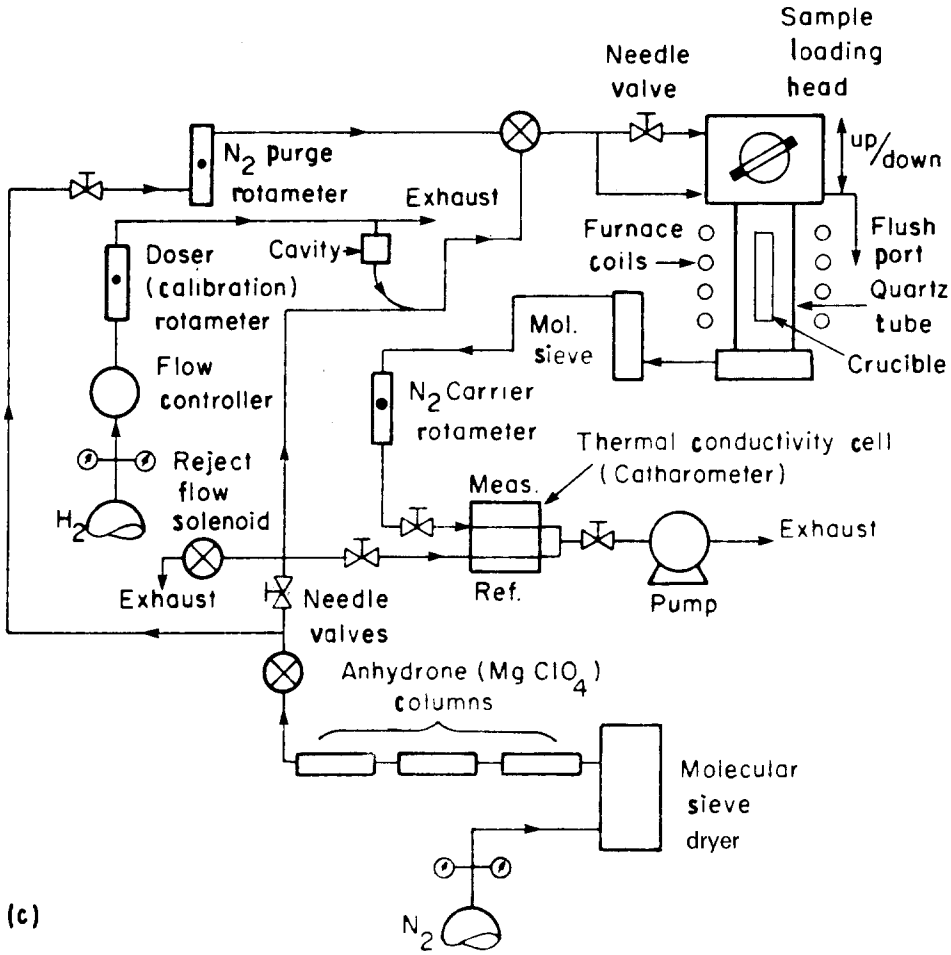

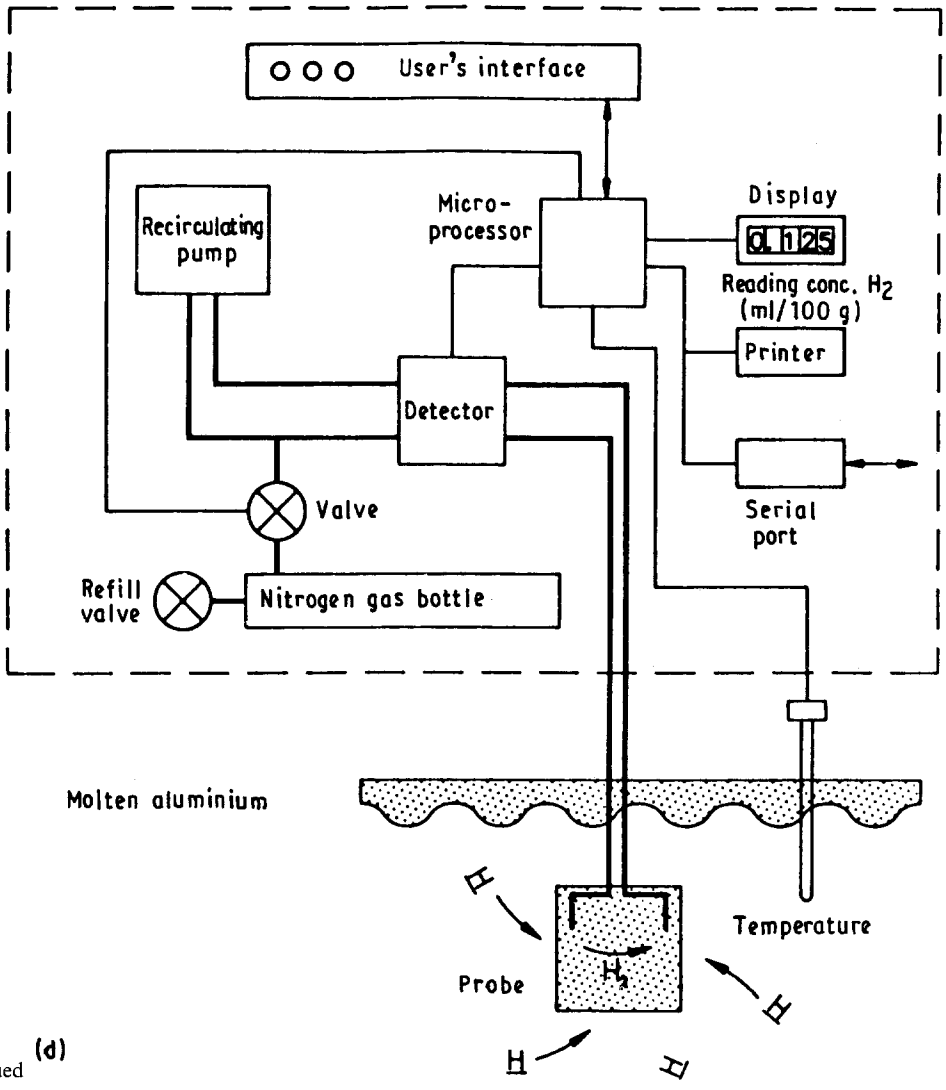

Figure 4 Continued

simple technique for on-line analysis of hydrogen in aluminium alloys [71]. Although based on the same operating principles as the original Telegas, several new features have been incorporated to increase adaptability to the cast-shop floor.

The design and material of the new "disposable" probe have been so chosen to enable it to overcome the problems associated with the ceramic probe and render it far superior to the latter. For full details of the probe, the reader is referred to Martin *et al.* [71]. Among its important advantages are that it can be used at any convenient angle, even in very shallow metal, and the need for bubbling gas into the metal is eliminated, thereby solving the blockage problem often associated with the original probe. However, to compensate for insufficient agitation of the melt (due to the absence of bubbling) which can lead to a much longer response time, a suitable movement is imparted to the probe.

A schematic diagram of the AlSCAN analyser is shown in Fig. 4d. Operation of the instrument is simple with the preselection of a specific number of parameters. According to extensive tests carried out at Alcan's Arvida R&D Centre, a comparison of Alcan probes, Telegas probes and the VSF technique showed that all three methods were more or less equally effective with differences in results being less than 0.02 ml per 100 g [72]. Reportedly, also, the comparative cost per analysis for the AlSCAN, NCF, Telegas and VSF techniques was 1:2:3:4.

4. Porosity

One of the biggest problems in aluminium castings is porosity, primarily caused by turbulent transfers during pouring of the molten metal. Apart from affecting the surface finish, porosity, in particular hydrogen-induced porosity, is always a cause for concern because it is detrimental to the mechanical properties.

The formation of porosity in solidifying metals can be attributed mainly to two effects: shrinkage, resulting from the volume decrease accompanying solidification, and the evolution of dissolved gases, resulting from the decrease in solubility of these gases in the solid as compared to the liquid metal [1, 77–86]. These effects may manifest themselves separately or, as is more often the case, simultaneously, interacting with each other to develop the resulting porosity observed. On account of this it is difficult, in most casting situations, to state which factor is predominant in causing the porosity. Precipitation of hydrogen in the solid state is also a third possible cause [1, 79].

A vast amount of theoretical work concerning the physics of pore formation as well as various experimental studies investigating the phenomenon have been reported in the literature [77–90]. Different types of porosity have been observed, mechanisms of pore formation suggested and models developed to substantiate them. In the following sections, an overall comprehensive treatment of these areas is given. However, in the present context of this article, hydrogen-related gas or microporosity is given main consideration throughout.

4.1. Formation of porosity

The shrinkage that occurs on solidification is the primary source of porosity formation in solidifying castings. In most cast alloys, the volume shrinkage varies typically from 5 to 8%. Shrinkage porosity also occurs on a "micro" level as "microshrinkage" or "microporosity" that is dispersed in the interstices of dendritic solidification regions, typically found in alloys with a large difference between their solidus and liquidus temperatures. Limited or inadequate liquid metal feeding in the dendritic solidification area is instrumental in the formation of this type of porosity.

The other main source of porosity arises from gas evolution resulting from a decrease in the solubility of the gas on solidification. The gas so rejected can nucleate both in the liquid during solidification and in the solid immediately afterwards, giving rise to two very different kinds of porosity, termed "interdendritic (or primary) porosity" and "secondary porosity", respectively. In addition, rejection of solute gas from the solid into the liquid continuously enriches the latter in the gaseous component. These effects are typically exhibited by hydrogen in aluminium. Both porosity types can significantly affect the casting. A detailed account of these porosities has been given by Talbot [1].

Nucleation of a gas bubble is necessary before gas porosity and its subsequent growth can occur. However, the large energy requirements for such nucleation are overcome by the formation of shrinkage porosity [77].

During the course of solidification, several types of feeding are involved at different stages of the solidification. These include liquid, mass, interdendritic and solid feeding, that occur from the initial through to the final stages of solidification. A schematic representation has been given by Campbell [88]. Porosity defects are caused by the limitations of these feeding mechanisms, and it is thought that the interdendritic feeding stage is the most important stage for their creation.

The growth process in porosity formation as given by Pehlke [77] is depicted in Fig. 5. In Fig. 5a, gas porosity is seen to nucleate at the base of dendrite arms. The synergism between the shrinkage and gas porosities overcomes the large negative free energy required to form a gas–metal surface, facilitating the nucleation as shown in Fig. 5a. As solidification proceeds, the porosity grows due to the higher potential for gas evolution. The radius of the porosity becomes large enough to decrease the contribution of interfacial energies, and the porosity detaches from the dendrite as shown in Fig. 5b, aided by convective

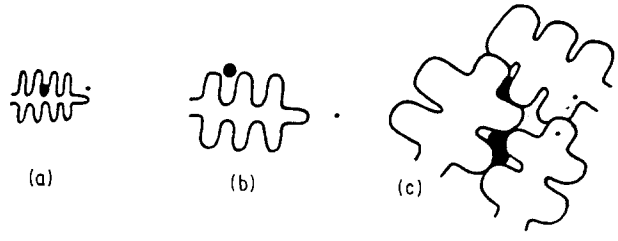

Figure 5(a–c) Growth process of porosity formation [91].

forces. At a still further stage of solidification, neighbouring dendrites collide, making interdendritic feeding difficult. At this stage, the porosity is thought to grow to compensate for solidification shrinkage (Fig. 5c).

According to Campbell [90], the conditions for the formation and growth of a pore are best given by

$$P_g + P_s > P_{atm} + P_H + P_{s-t}$$

where P_g = equilibrium pressure of dissolved gases in the melt, P_s = pressure drop due to shrinkage, P_{atm} = pressure of the atmosphere over the system, P_H = pressure due to the metallostatic head and P_{s-t} = pressure due to surface tension at the pore–liquid interface.

It is generally observed that P_g and P_s are the major drawing forces, acting synergistically to form pores within the interdendritic regions that are neither solely due to gas evolution nor due to shrinkage. For a particular casting design, P_{atm} and P_H are constant, and a decrease in P_{s-t} (as has been observed for modifiers like sodium [46]) can lead to an increased probability of pore formation.

4.2. Hydrogen-related gas porosity and microporosity

Being the only gas soluble in aluminium alloys, hydrogen is the main contributor to porosity in these alloys. When the hydrogen content of the melt exceeds the solubility limit, the resultant excess hydrogen forms gas bubbles, leading to porosity. The pores nucleate and grow in the presence of proper nucleants [92, 93], their size and distribution depending on the local solidification conditions [1, 85]. The porosity formation is described by the relation $\Delta P = 2\sigma/r$, where σ is the surface tension and ΔP is the critical pressure that must be exceeded in the pore for a pore nucleus of radius r to grow. A higher hydrogen concentration in the melt will increase ΔP and decrease r, resulting in an increase in the amount of porosity in the casting [46, 94]. Pores may form either prior to or during solidification. Pores of the former type are spherical and relatively large. The ones formed during solidification are small, irregularly shaped and attributed to shrinkage porosity. Their formation is influenced by the hydrogen enrichment and the shrinkage pressure in the interdendritic area [87].

A number of models have been developed for the nucleation and growth of gas bubbles during solidification [91, 95–97]. Most models assume that a bubble forms and grows after a critical gas concentration is reached locally in the liquid, usually between dendrites or near grain or cell boundaries. For any given alloy and specific solidification condition, there is a "threshold hydrogen content" below which no primary porosity is formed.

Hydrogen gas porosity has been extensively investigated. In general, this has been done using directional solidification techniques. It has been established that, in addition to the threshold hydrogen content mentioned above, the tendency for porosity formation is reduced with an increase in cooling rate and a decrease in alloy freezing range. Also, for hydrogen contents above the threshold value, there is approximately a linear relation between hydrogen and pore volume fraction [82].

The formation of different types of microporosity has been dealt with by various workers [91, 94, 95]. It is found that porosity increases with distance from the chill to the casting [46, 98, 99]. In spite of various mechanisms that have been proposed [46, 81, 90] for the nucleation of porosity in Al alloys, only the simpler ones are used in mathematical modelling.

According to Kubo and Pehlke [91, 100], formation of porosity in solidifying alloys is enhanced by gas evolution and by interdendritic flow in the later stages of solidification. They have developed a mathematical model for the same that suggests that the simultaneous occurrence of shrinkage and gas evolution is an essential mechanism in the formation of porosity defects. Measured values of porosity in Al–4.5% Cu plate castings compare favourably with their calculated values. They recommend minimization of gas content by degassing and increasing the mould chilling power for the production of sound castings. Actual recommended values would depend on the casting shape, alloy composition and required mechanical properties, among other variables.

As part of an ongoing research programme on the solidification characteristics of Al alloy castings, the research group of the Aluminium Casting Research Laboratory (ACRL) at Drexel University, Philadelphia, has been investigating microporosity formation in such castings. The effects of various casting parameters (including cooling rate and initial hydrogen content) on the microporosity have been studied. Porosity and shrinkage defects ensue as a result of inadequate feeding of the metal and the voids caused by the dissolved hydrogen liberated from the alloy during solidification. The solidification shrinkage and gas generation combine in the interdendritic regions giving rise to the observed microporosity.

From the same group, Zou *et al.* [101] have investigated the fundamental mechanisms associated with microporosity formation in the solidification of A356.2 castings. Their experimental results on simple test castings of the alloy show that the pore density is essentially constant for various hydrogen concentrations, while the pore size and amount of porosity increase with the initial hydrogen content in the liquid metal. Based on their results, they have developed a micromodel to simulate microstructure evolution and porosity formation in equiaxed structures, which incorporates the effects of hydrogen liberation at the metal front and that of interdendritic fluid flow.

The measured and calculated amount of porosity as a function of initial hydrogen content as obtained by them [101] is reproduced in Fig. 6. As observed, there is a linear variation between the amount of porosity and the initial hydrogen content. Experimental data from other sources are also included in the figure for comparison. The overall agreement lends support to the validity of their model.

Poirier *et al.* [95] have analysed the microporosity observed between primary dendrite arms. This type of

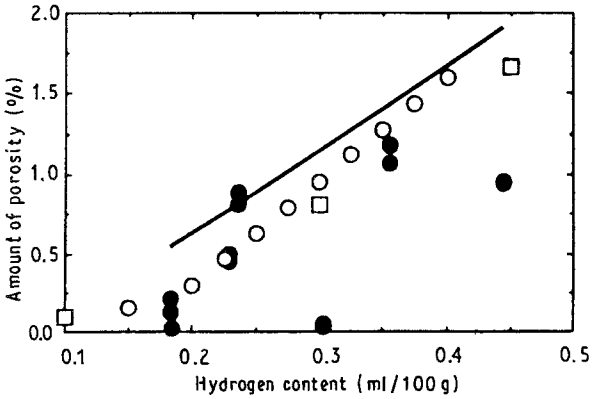

Figure 6 (●) Measured and (——) calculated amount of porosity in A356 alloy as a function of initial hydrogen content at $dT/dt = 2.5\,^{\circ}C\,s^{-1}$ (from Zou *et al.* [101] together with data of (□) Thomas and Gruzleski [82] and (○) Deoras and Kondic [102].

porosity is often found in alloys which possess a fully developed dendritic structure at a low solid fraction and also sometimes in directionally solidified eutectics. Uniform hydrogen content in the liquid and solid phases and an interdendritic fluid flow directed by d'Arcy's law are among some of the assumptions used in their analysis. Their results indicate that porosity does not form when the gas pressure is below the pressure in the liquid and that it is proportional to primary dendrite arm spacing.

On the basis of thermodynamic data and observed aspects of dendritic solidification, Poirier *et al.* have predicted the formation of interdendritic porosity in directionally solidified Al alloys. Their model calculates the pressure of hydrogen within the interdendritic liquid and if this pressure is higher than the sum of the local and capillary pressures, then the formation of interdendritic porosity is possible. A gas pore is stable provided that

$$P_g - P = \sigma\left(\frac{1}{r_1} + \frac{1}{r_2}\right)$$

where $P_g - P$ represents the local pressure within the mushy zone, σ the surface tension and r_1, r_2 the principal radii of curvature. In a columnar mushy zone, the widths of the spaces between the primary arms being greater than those between the secondary arms, less excess pressure is needed for a gas pore to exist in the former than in the latter. Thus Poirier *et al.* recommend that

$$P_g - P = 4\sigma/g_L d_1$$

g_L being the local volume fraction of liquid and d_1 the primary dendrite arm spacing. Their equation predicts that a stable gas pore which forms during the later stages of solidification requires a relatively high excess pressure. Their predicted values of porosity as a function of initial hydrogen concentration agree well with their experimental data.

Fang and Granger [94] have proposed a mathematical model to predict the size of interdendritic pores that form in the interdendritic regions between equiaxed grains. Their model describes the growth of pores during solidification and examines the effects of hydrogen content and solubility, dendrite cell spacing and local solidification characteristics on the pore size. The model is based upon a mass balance between the amount of hydrogen entering a pore and that rejected at the solidification front. According to them, alloy composition, processing variables, hydrogen concentration, grain refining and inclusion content are the five factors that control porosity formation, and to date there is no one consistent model that accounts for all these aspects of the porosity phenomenon. Their model is aimed at taking a step in this direction. The authors report that the predictions of their model agree, in general, with reports on gas porosity given in the literature. Fig. 7 is a schematic representation of pore formation in an equiaxed-grain casting produced by directional solidification as given by them.

Among the conclusions derived from their computational results are that the pore size decreases with decreasing hydrogen content and with increasing hydrogen solubility, increasing hydrogen partition coefficient and increasing external pressure. Pore size is affected by the cooling rate in the sense that the latter affects the local solidification structure (i.e. the dendrite cell spacing) which in turn controls the threshold cell size and hence the pore size. Also, there exist a critical hydrogen content for a given alloy below which no pores form, as well as a critical external pressure above which pore formation may be suppressed.

At this stage, in connection with what has been said above, it is of interest to point out that, while many investigators treat ingot porosity only in terms of the mean porosity, such mean values can be in considerable error and provide a very unreliable picture, since the porosity can vary considerably from the mean value at various points within the ingot. In this regard,

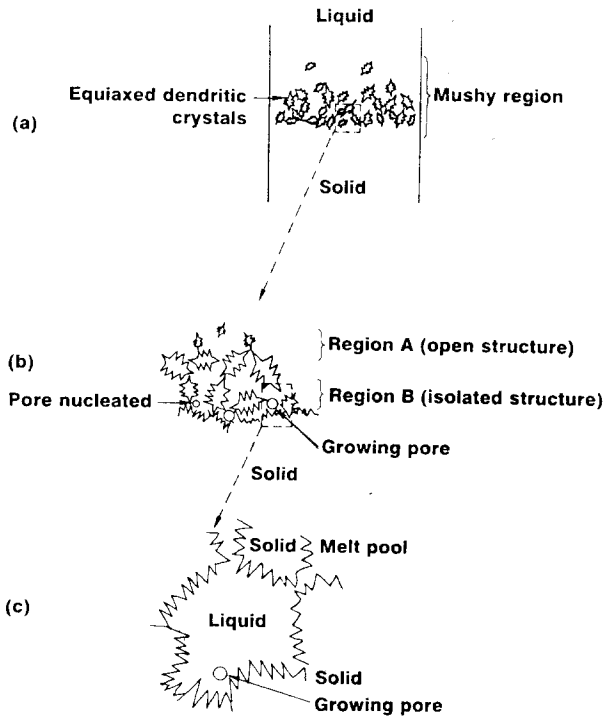

Figure 7 Schematic representation of pore formation process in an equiaxed-grain casting obtained by directional solidification [94].

Entwhistle *et al.* [103] have carried out studies to determine the development and distribution of porosity in Al-base (Al–4.5% Cu and Al–8% Si) alloys. According to them, a definite pattern of microporosity exists over a wide range of casting conditions and hydrogen concentrations, which can be interpreted in terms of the solidification of the ingot. At very high gas levels (> 0.7 ml H_2 per 100 g Al) the pattern disappears and the porosity becomes uniform throughout the ingot. At very low levels (< 0.1 ml H_2 per 100 g Al) the porosity pattern again "disappears", in that it is not readily detectable. Khomitskii [104] has also alluded to this fact in his work on porosity evaluation in castings.

4.3. Effect of modification

The influence of modification on porosity is a matter of considerable debate, stemming, in the main, from the controversy over the behaviour of Sr as a modifier. As has already been discussed in detail above, the modifier is weighed in terms of its role in enhancing the susceptibility to hydrogen pick-up of the modified alloy, which, in turn, directly bears upon its porosity content. It would appear to be the foregone conclusion, in the case of such modifiers, that an increase in porosity (both gas and microporosity) would result, depending on the interdendritic feeding ability in a particular local solidifying region of the alloy. What concerns the casting industry is whether modifiers increase the amount of porosity present in the final product, since it is generally observed that modified castings contain more porosity than unmodified ones.

Among the several authors [31, 46, 105–108] who have reported either an increase or else no increase in hydrogen gas levels with the addition of Sr, the work of Shahani [46] is of particular interest in the present context. Investigating the effect of hydrogen on the shrinkage porosity of Al–Si alloys, he found that addition of Sr or Na actually reduced the gas content but, however, increased the porosity of the modified casting. According to him, the amount of shrinkage porosity in castings is determined by the gas content, the pressure drop caused by shrinkage and the foreign particles present in the melt. Modifiers promote this type of porosity, facilitating the nucleation of pores by reducing the surface tension or by acting as nucleants.

Denton and Spittle [31], in their investigations on the effects of Sr addition on hydrogen susceptibility in Al–Si LM6-type alloys, found that Sr enhanced the said susceptibility and that there was a direct correlation between porosity and measured hydrogen concentrations. Examination of the graphite mould chill castings obtained from LM6 melts modified with 0.01% Sr showed that the gas porosity tended to increase towards the centre. Fig. 8 depicts the percentage porosity versus hydrogen concentration obtained by them. As can be seen, there appears to be a cut-off hydrogen concentration of about 2 $mm^3 g^{-1}$ below which it was difficult to detect porosity. Similar results have been described in the previous section (see also Fig. 6).

Argo and Gruzleski [107] have summed up the controversial situation regarding modification: it is natural to attribute increased porosity in modified castings to an increased hydrogen content, the modifier being thought to be somehow responsible for increasing the susceptibility of the melt to hydrogen pick-up. However, their group [45, 108] has shown that, at least in the case of Sr, this is not the case. In the absence of such a connection, it becomes more difficult to explain the tendency of modified castings to exhibit greater porosity. These authors have therefore carried out a controlled study on porosity in modified and unmodified A356 alloy, using the Tatur test to identify differences in the distribution of porosity and shrinkage. This specialized test measures the various types of shrinkage found in foundry alloys. Their radiographic data and Tatur results have shown that modification leads to a redistribution of porosity on solidification, from primary pipe type into microporosity, appearing thereby to "increase" the porosity. The results of Charbonnier *et al.* [33] on a similar study of Na-modified AS7G alloy appear to agree well with their results. The increased microporosity is a result of the increased difficulty in feeding during solidification, and appears to be a basic feature of the modification process, related to the increased freezing range of modified alloys. According to them, there is now growing evidence [93, 94, 109] to indicate that at equal levels of hydrogen, a modified casting does indeed contain more microporosity than an unmodified one, and the increase is due to the above-mentioned

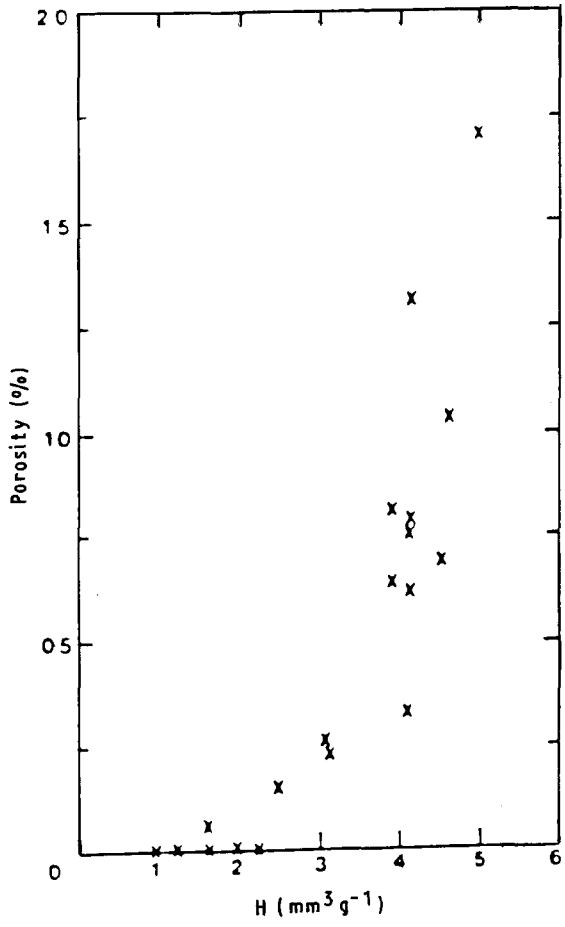

Figure 8 Percentage porosity vs hydrogen concentration [31].

redistribution of porosity type. Both the freezing range and the microscopic shape of the eutectic solid–liquid interface determine the final pore size and shape. It has been observed both by Argo and Gruzleski [107] and Fang *et al.* [78] that micropores in modified alloys are larger than those in unmodified alloys.

According to Argo and Gruzleski, in ummodified alloys the eutectic exhibits an irregular solid–liquid interface, because of which small pockets of liquid are entrapped between advancing solidification fronts, resulting in fine concentrated microporosity, whereas in modified alloys, a regular or planar interface results in a more widely dispersed and larger porosity. Other workers [78, 110, 111] have also reported similar observations.

Sigworth *et al.* [112] agree in principle that modification affects the shape of the solid–liquid interface and that unmodified castings have been known to exhibit concentrated "spongy" shrinkage areas that become sound when modified. However, they have reservations about the tests performed by Argo and Gruzleski [107] in that the latter authors did not employ a riser in the Tatur mould, their experiments were conducted at relatively high gas concentrations (which would be expected to worsen the observed porosity problems) and they did not grain-refine their samples. In the opinion of Sigworth *et al.*, proper precautions taken in these areas can eliminate undesired porosity to a large extent. Reduction of gas content, proper mould design and modification combined with grain refinement are expected to produce the best results.

Recently, Iwahori *et al.* [113] have shed more light on the occurrence of porosity in Na- and Sr-modified Al–Si alloys, from the viewpoint of oxide inclusions and hydrogen content present in the melt. Porosity occurs due to the increase in hydrogen content of the melt when these modifiers are added. However, while the hydrogen content in unmodified or Na-modified melts is readily decreased by vacuum degassing, that in an Sr-modified melt is not. It is also observed that when a melt without oxide inclusions is degassed in vacuum after the addition of Sr, no porosity is found to occur [114]. Thus, it is the oxide inclusions in the melt that are responsible for reducing the rate of hydrogen degassing in vacuum and that facilitate the occurrence of porosity in the casting. The hydrogen absorbed by the oxide inclusions present in the melt is more strongly fixed in them by the addition of Sr to the melt. Typically, for a general case of melting, as many as 35 inclusions per 500 mm^2 may be present. With Sr addition, the number is further increased, while vacuum degassing ($\sim$ 20 min) reduces the number to about one-third. No inclusions occur in castings to which an NaCl–25% AlF_3 flux inclusion removal treatment is applied. Fig. 9 shows the amount of porosity as a function of hydrogen content in unmodified and modified Al–7% Si alloys as obtained by these authors. The linear relationship is again observed.

In contrast to the findings of Closset and Gruzleski [109], but in accordance with the reportings of Shahani [46], these authors have observed that porosity occurred with a lower hydrogen content for the Sr-modified alloys. In their opinion, this indicates that Sr is more sensitive to the occurrence of porosity.

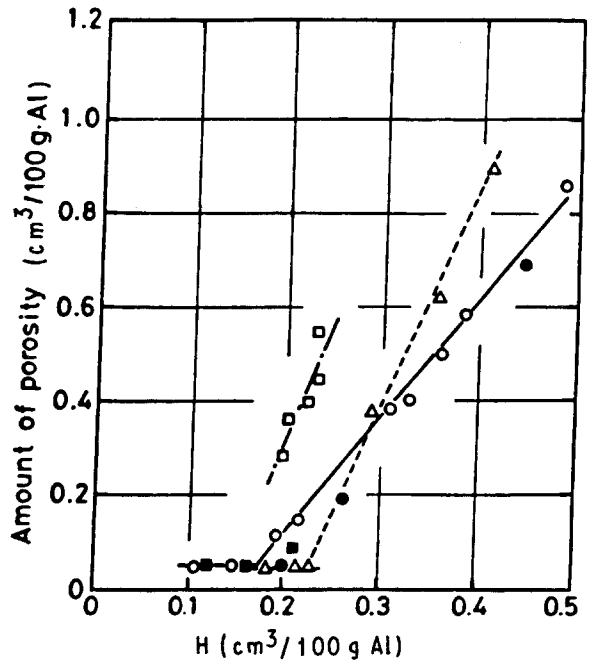

Figure 9 Amount of porosity as a function of hydrogen content in unmodified and modified Al–7% Si alloys [113]. Inclusion removal treatment: (●) unmodified, (■) Sr-modified. No treatment: (○) unmodified, (□) Sr-modified, (△) Na-modified.

They have also investigated the feeding ability of the modified alloys. Na is found to improve the feedability and can produce sound castings free from shrinkage porosity. Sr, on the other hand, has no such effect on the alloys, in that it does not decrease the shrinkage porosity nor increase the feedability [114].

It is interesting to compare the results obtained by them on the density distribution of unmodified Al–7% Si alloy castings as a function of the distance from the bottom of the casting to the riser with those obtained by Argo and Gruzleski [107] for unmodified and Na/Sr-modified A356 sand-cast bars of the same composition, as a function of distance from the graphite chill end used in their investigations. These are given together in Fig. 10a and b to facilitate comparison.

Bearing in mind the high hydrogen content in the melt prior to degassing, the related porosity that occurs will lower the density of the casting as a whole. Upon vacuum degassing, the densities of the upper and lower sections of the casting will increase due to the removal of hydrogen-related gas porosity, while that in the central region will decrease due to a concentration of the shrinkage porosity in this area that is the last to be solidified–hence the curves observed in Fig. 10a.

Comparing Fig. 10a with the results of Argo and Gruzleski (Fig. 10b) and with the experimental data of both groups, the curves obtained by both for the unmodified alloy are reasonably similar. In Fig. 10a, the vacuum degassing of 20 min corresponds to a hydrogen content of approximately 0.18 cm^3 per 100 g Al, which is close to the 0.200 $\pm$ 0.007 cm^3 per 100 g Al value obtained by Argo and Gruzleski for

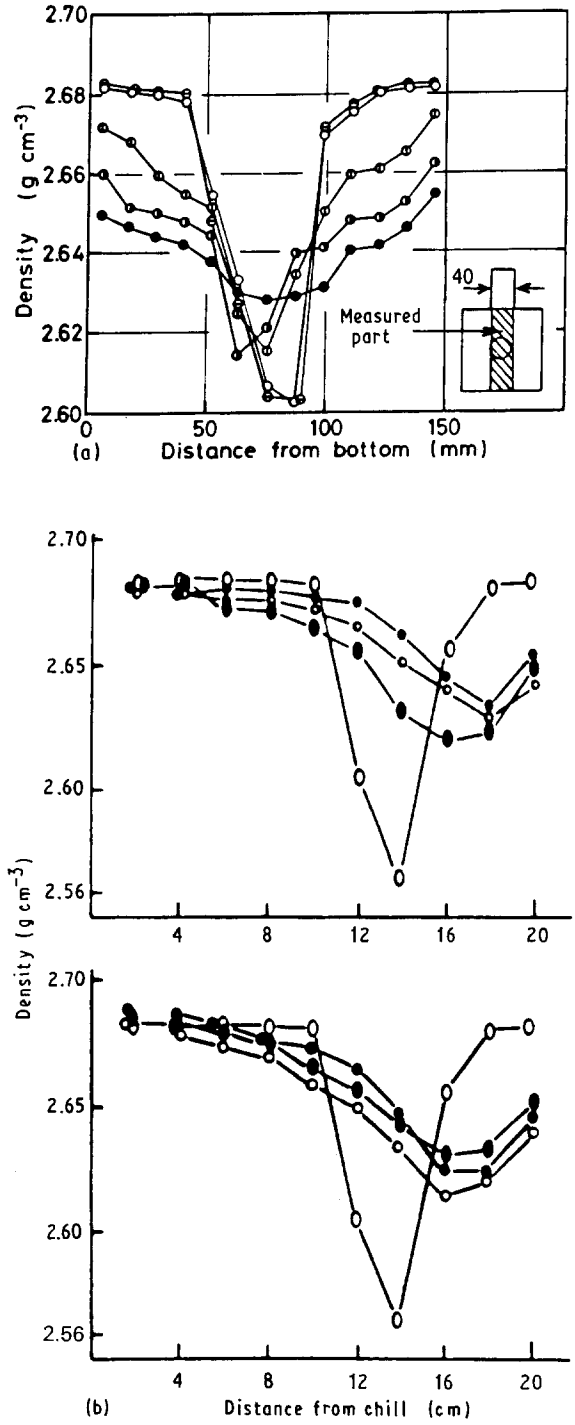

Figure 10 (a) Variation of density versus distance from bottom for vacuum-degassed unmodified Al–7% Si alloy castings [113]. Vacuum degassing time: (●) O min, (◑) 5 min/1.0 torr, (Φ) 10 min/0.6 torr, (○) 20 min/0.3 torr, (⊖) 40 min/0.26 torr. (b) Variation of density from graphite chill for Sr and Na-treated bars of Al–7% Si alloy [107]. Upper plot: (○) 0 Sr, (◐) 0.003 Sr, (○) 0.009 Sr, (●) 0.012 Sr. Lower plot: (○) 0 Na, (◐) 0.002 Na, (○) 0.003 Na, (●) 0.012 N.a.

their unmodified alloys after subjecting them to degassing treatment with argon. Also evident in Fig. 10b is the smoothing effect of Na or Sr modification on the overall porosity distribution.

It is interesting to note that, while there is an overall agreement of the curves obtained by the two groups for the unmodified alloy, Iwahori's group has stressed the importance of the use of an appropriate riser in the solidification of the castings to minimize the occurrence of shrinkage porosity, whereas Argo and Gruzleski did not use one in their experiments (as pointed out by Sigworth *et al.* [112]). According to Iwahori *et al.* there is a minimum or "requisite riser size" for these alloys, required to produce defect-free (without shrinkage porosity) castings. The smaller the size, the more effective the feeding. In Al–Si alloys, due to the lowering in the feedability with increasing Si content, the riser size increases for alloys with higher Si contents.

As far as modification is concerned, the requisite riser size of Na-modified alloys is remarkably small, while that of Sr-modified alloys can go up to 100 mm. Thus, modification with Na greatly enhances the feedability of these alloys, whereas Sr has virtually no such effect.

The importance of risers in the solidification process is also evidenced by the recent work of Lee *et al.* [115] who have reported on the feeding behaviour during solidification of Al–7Si–0.3 Mg alloy plate castings. Investigating the systematic change of riser size and casting geometry by thermal analysis, they have modelled the interdendritic feeding behaviour in the alloy, and obtained a new feeding efficiency parameter, $(Gt^{2/3})/V_s$ (where G is the thermal gradient, t is the local solidification time and V_s is the solidus velocity), which integrates all individual thermal variables and is found to satisfactiorily predict the formation of porosity. According to them, the combined geometries of a casting and its riser size exert a great (and complicated) influence on the thermal variables of the alloy, which synergize to govern the feeding behaviour of the casting. More significantly, they find that the applicability of D'Arcy's law (which has been generally thought to govern interdendritic fluid flow in porous media) depends on the regime of solidification time and is only applicable to certain thermal conditions in the solidifying casting.

Michels and Engler [116] have also reported on the effects of alloy content, modification, refinement and casting geometry on the feeding characteristics and porosity of Al–Si alloys.

Tuttle *et al.* [117] have studied the effect of Sb on A356 Sr-modified Al melts. According to them, the Al–Si eutectic obtained by additions of Sb is not a "modified" one but, rather, a "refined lamellar" type of structure (as compared to the "fibrous" structure of Na- and Sr-modified alloys or the "acicular" one obtained with P additions [118]). They have found that the Sb-refined alloy does not exhibit a marked tendency towards microshrinkage, unlike that obtained with Sr modification.

Alloy modifications have also been done using P in the form of phosphides of copper, boron and zinc. Modifying with phosphides does not in general influence the eutectic, but leads, rather, to a reduction in the primary Si particle size [119–121]. While Carlson and Pehlke [122] have obtained a relation between the quality index factor Q and the porosity and phosphorus level for A390 alloys, the correlation, as expected, is not a strong one as the properties are affected by several other factors besides the porosity and phosphorous contents.

4.4. Effect on mechanical properties

Alloys of the Al–Si–Mg system, in particular A356 and A357, have been the subject of extensive research because of their commercial and technological importance. They are very similar in composition and vary mainly in their magnesium contents. A higher Mg content increases the capability to harden the alloys (due to precipitation of magnesium silicide, the precipitate responsible for hardening) while the mechanical properties are affected appreciably by the morphology of the Si in the alloy matrix. Modification (with Na or Sr) changes the Si morphology to a fine fibrous form that results in an improvement of the mechanical properties.

While the mechanical properties are determined by several processing parameters, including alloy composition as described above, only those will be considered here that are directly or indirectly related to the occurrence of porosity. Porosity is determined or affected by the hydrogen content of the melt and the presence of inclusions, and the modification and/or grain refinement applied to the melt. Local solidification time is a major factor determining the amount of porosity, along with the alloy composition and the casting design.

That porosity will affect the mechanical properties is to be expected, porous structures being weak and brittle as opposed to the strength and ductility of dense structures. Large variations in yield strength, ultimate tensile strength and elongation values have been observed and have been attributed to microporosity. Fig. 11 is a typical photomicrograph of A356 Al alloy showing the appearance of micropores. The phase change from liquid to solid alloy is accompanied by a 7% volume reduction. When there is insufficient "feeding" to compensate for this volume change microporosity occurs and prevents the attainment of peak properties.

It has been observed that interdendritic porosity that is present in ingots cast for fabrication is flattened into planar discontinuities in the course of working operations [123, 124]. In thick plates and forgings, this leads to a reduction in the mechanical properties in the direction normal to the direction of working. Turner and Bryant [124] measured the tensile properties of plates hot-rolled from semi-continuously cast ingots of a high-strength Al–Cu–Mg–Si alloy. Their results gave good correlations between these properties and the hydrogen porosity in the ingots. Some of their results are illustrated in Fig. 12. Similar effects have been reported in Al–Zn–Mg–Cu alloy forgings [125], where it was found that the weakness induced by porosity was associated with a change in the fracture path from transgranular to intergranular.

According to Stein [126], there are four factors that influence the mechanical properties: composition and heat treatment, that have a general influence, and rate of solidification and integrity of the cast structure, that affect specific areas of a casting. The first two affect the strength level of the matrix in that the strength decreases if these factors are not at their highest level. When the other two are less than ideal, microporosity occurs and there is a decrease in the mechanical properties.

As mentioned earlier, the grain refinement applied to a melt also affects the porosity. According to Sigworth [127], among the several advantages of grain refining, the primary one is an improvement in the amount and distribution of porosity and shrinkage in alloys which tend to form microporosity, especially those with a long freezing range [127, 128]. This results in a significant improvement in the mechanical properties of the casting [129, 130], especially under fatigue loading, since fatigue failure in Al alloys is intergranular [131]. Grain refining will also reduce the amount of porosity found in an alloy containing small or moderate amounts of gas [132].

In the case of modification, the enhancement in mechanical properties can easily be offset by the tendency for increasing the porosity in the modified casting. The presence of porosity in the casting induces tensile transverse stresses in Si particles and at the particle–matrix interface [133]. These stresses promote crack initiation and thus lower the mechanical properties. Porosity levels in excess of 1% significantly reduce tensile properties, especially the percentage

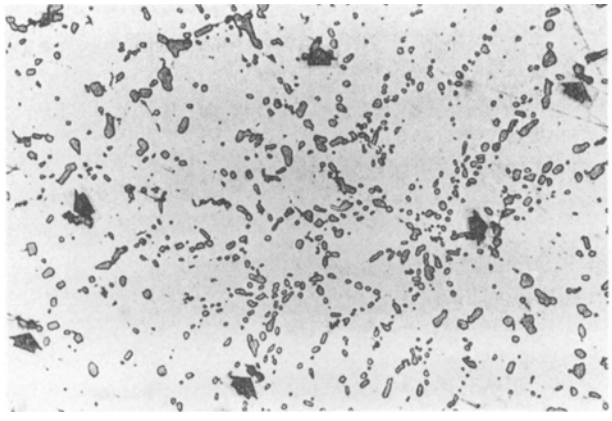

Figure 11 Typical photomicrograph of A356 Al alloy showing the presence of micropores [126].

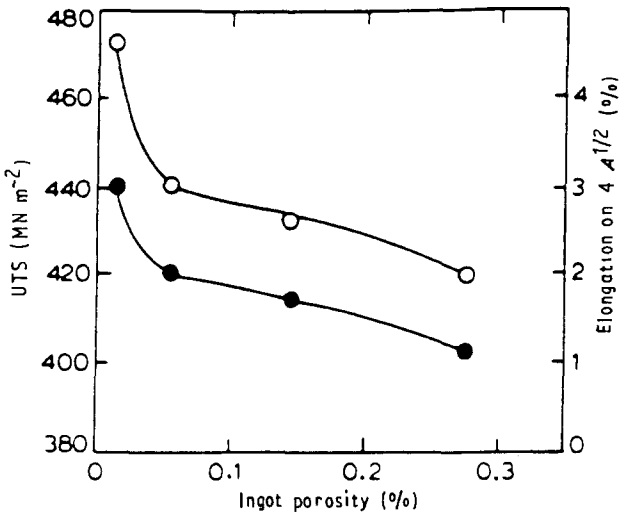

Figure 12 Effect of ingot porosity on the tensile properties of plates hot-rolled from semicontinuously cast ingots of a high-strength Al–Cu–Mg–Si alloy [124]: (○) UTS, (●) elongation.

elongation. Shivkumar *et al.* [134] obtained typical porosity contents of 1 and 1.75% respectively in unmodified and modified sand-cast bars of A356.2 alloy, amounts generally observed in commercial castings. Their results showed that, despite the introduction of porosity, modified samples showed appreciably higher tensile properties than the unmodified ones.

The property that was most affected by modification (and solution treatment) was the percentage elongation, with modified bars possessing a higher elongation than unmodified ones. The fracture mode changed from brittle to ductile upon modification in the case of sand-cast samples, while permanent-mould castings exhibited a ductile fracture in both modified and unmodified specimens.

Another investigation on the fracture behaviour in modified Al–7% Si–0.3% Mg alloy has shown that fracture takes place in a transgranular fashion and also confirms the ductile nature of the fracture from the characteristic dimple-like patterns observed on the fracture surfaces of the cast alloy [135]. Thus, modified alloys possess higher ductility than unmodified ones [136].

Kutsenok *et al.* [137] have investigated the formation of porosity in Sr- and Zr-modified hypoeutectic AL9-1 alloys of aluminium. Voids observed by scanning electron microscopy at fractures in their permanent-mould cast specimens display characteristics of dispersed shrinkage porosity. The Sr modification leads to microshrinkage, while the addition of Zr to the Sr-modified alloy somewhat reduces the tendency for the formation of microshrinkage porosity. However, increasing the Zr content leads to embrittlement. In their investigation, alloy specimens containing 0.04% Sr and 0.08% Zr were found to exhibit an increase of about 22% in the porosity area observed on the fracture surfaces of these specimens, which resulted in reductions in the tensile strength and plasticity. Similar studies on the evaluation of casting defects in Al–Si alloys by SEM have been carried out by Reznicek and Holmanova [138].

Ohsasa *et al.* [99] have reported the occurrence of plate-like and globular porosities in fracture surfaces of undirectionally solidified Al–1% Si and Al–3% Si alloys, respectively. The mechanical properties of the alloys were evaluated by means of the bending test. Fig. 13a shows the relationship between porosity and bending strength for the Al–Si alloys as obtained by them. Taking into account the scatter in the data, for a higher Si content the bending strength apparently decreases more rapidly with the increase in porosity content, while for a lower Si content the changes are not that well defined.

Another example of the deleterious effect of hydrogen content on mechanical properties is shown in Fig. 13b as obtained by Traenkner [139] for sand-cast 356-T6 aluminium castings.

As some porosity (2–4%) almost inevitably occurs in all castings, it seems reasonable to anticipate an acceptable level of porosity for a particular casting. Eady and Smith [140] carried out investigations along these lines, to assess the effect of relatively small levels of porosity (normally present in "sound" castings) on the mechanical properties of a casting. They chose to investigate alloys based on the 601 composition but with Mg content varying from 0.1 to 0.5 wt %. They found that, in general, the UTS, proof stress and elongation decreased with increasing porosity (Fig. 14). However, the magnitude of the effect of porosity was controlled by the Mg content of the alloy (Fig. 14a and c).

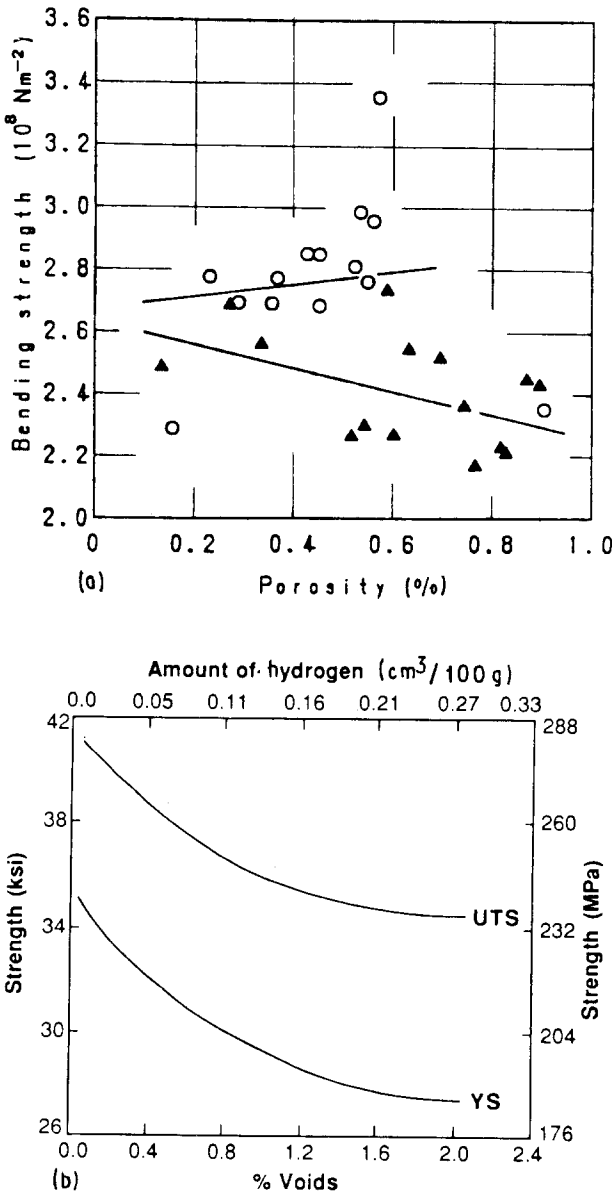

Figure 13 (a) Porosity versus bending strength for Al–Si alloys [99]: (○) 1% Si, (▲) 3% Si. (b) Effect of hydrogen porosity on the tensile and yield strengths of sand-cast 356-T6 aluminium castings [139].

The pore shape was not found to have any significant effect on the measured tensile properties. According to them, the effect of porosity on 601-type alloys is not straightforward and can be masked or directly affected by variations in Mg content or the dendrite arm spacing (DAS). These parameters can produce variations in UTS and proof stress that far outweigh the effects of porosity. Porosity, however, can have a large effect on ductility, even very small levels being extremely detrimental when the alloy possesses a reasonable inherent ductility. With respect to tensile properties, porosity can be responsible for altering the stress field to initiate fracture, thus affecting crack

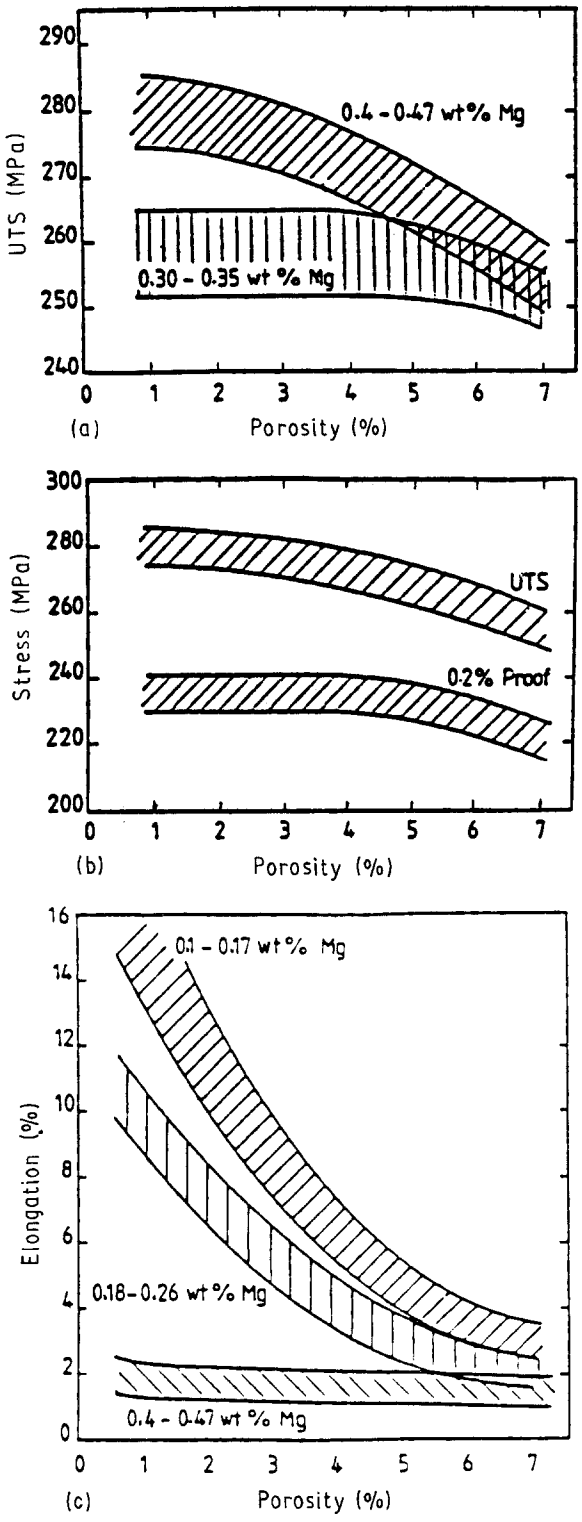

Figure 14 Variation of mechanical properties with porosity content in CP601 type Al alloys (DAS 33–37 μm): (a) UTS, (b) stress (0.40–0.47% Mg), (c) elongation. After Eady and Smith [140].

propagation. Examinations of the fractured specimens confirm the trends observed in the mechanical properties as a function of porosity.

Overall, the work of Eady and Smith shows that it is difficult to specify an acceptable level of porosity for any given casting without also specifying other parameters that affect the ductility. In their opinion, porosity levels of 2–3% should not, in general, be significant with respect to the tensile properties and in some cases, levels of even up to 7% might also be of little consequence.

4.5. Advantage of porosity

From the many investigations on porosity and its distribution in a casting, various pore-free casting technologies have been developed [141–143] to keep porosity levels to a minimum. As already mentioned above, some porosity, however, is almost inevitable in all castings, and it has been found that the effect of porosity is not always detrimental to their tensile properties. Eady and Smith [140] have shown this to be the case, and according to them, porosity levels of 2–3% are not significant in most cases. In fact, well-dispersed hydrogen porosity is not always undesirable because it can be used to balance solidification contraction and help prevent the greater damage caused by localized shrinkage cavities [1, 144]. This is done by deliberately introducing the hydrogen into the molten metal before casting [1, 145, 146]. The practice must be carefully controlled and applied with discrimination because even dispersed porosity can adversely affect the mechanical properties of the casting [147–150] to an extent depending on the nature of the alloy. For example, the properties of castings of general-purpose Al alloys are not unduly affected by moderately high hydrogen contents because the gas voids form in the eutectic part of the alloy and are round-shaped [147]. In contrast, the mechanical properties of a high-strength Al–10% Mg alloy are very sensitive to gas porosity because it forms in layers [150].

Afanas'ev and Prudnikov [146] have found that hydrogen acts as a modifier which alters the microstructure in Al alloy (Al–Cu and Al–Fe) castings in a manner leading to higher strength and ductility. A finer eutectic structure can be brought about by the presence of hydrogen. The charge preparation treatments (hydrogenation in the molten state followed by pasty-state working) proposed by them are found to help in regulating the hydrogen content of the poured metal and may therefore be regarded as a practical means of controlling hydrogen and its effects on structure and properties. They report that working the charge materials in the pasty state increases the UTS of the casting by about 50% for Al–Cu alloys, while preliminary hydrogenation before working in the pasty state produces a further increment of 20–30% in the UTS and 15–40% in the elongation.

Tiwari *et al.* [144] have studied the effect of hydrogen gas content on shrinkage defects in a series of Al–Cu and Al–Si alloys with varying hydrogen contents. They found that, depending on the alloy composition, a certain volume of hydrogen gas needed to be introduced into the molten alloy to counteract the shrinkage defects and form uniformly dispersed gas holes in the casting. The amount of hydrogen gas needed showed a correlation with the liquidus temperature of the alloy. Representative photographs of longitudinal sections of some of these alloy castings are given in Fig. 15. It is seen that, irrespective of the mode of solidification, all the alloys show that at a certain gas content, the major shrinkage defect (pipe or cavity type) occuring at the lowest gas content in the casting is replaced by uniformly dispersed gas holes.

Surappa *et al.* [151] have studied the effect of macroporosity on the strength and ductility of gravity

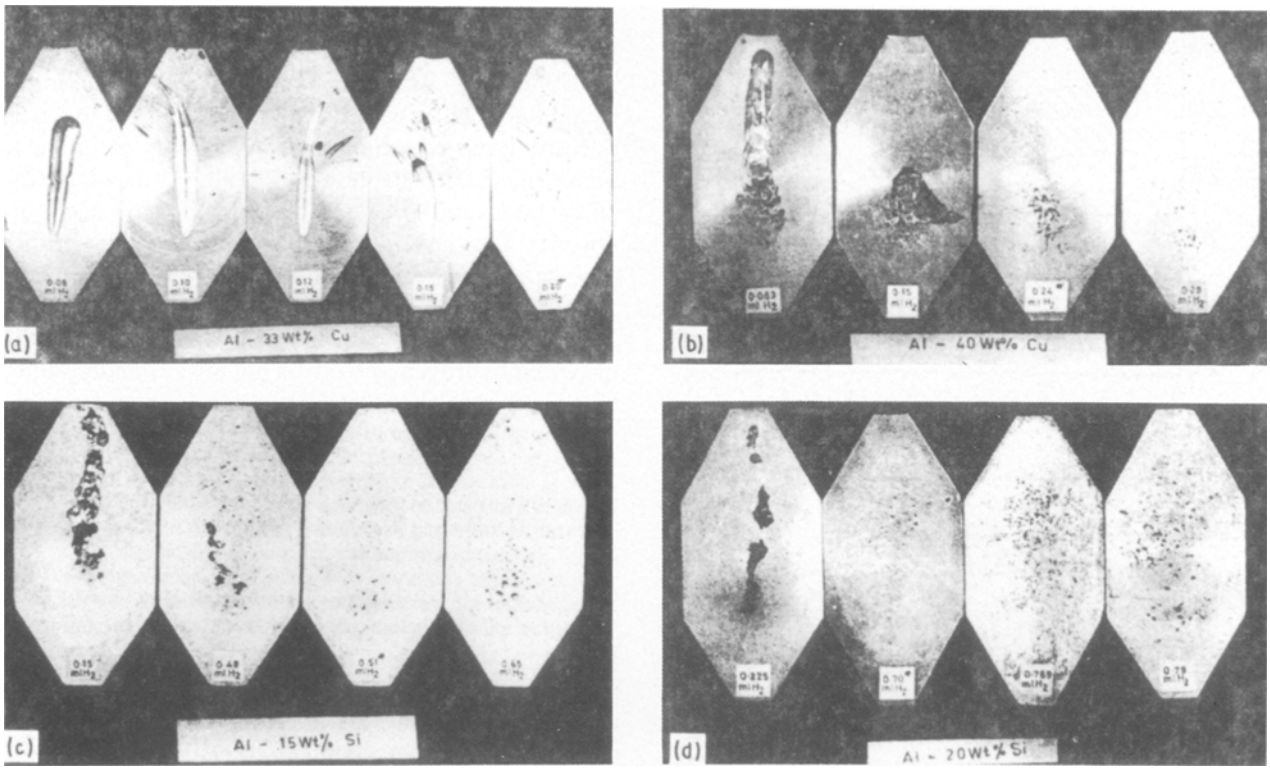

Figure 15 Longitudinal sections of (a, b) Al–Cu and (c, d) Al–Si alloy castings with varying hydrogen gas content [144].

die cast Al–7Si–0.3 Mg alloy. The micrograph of a typical test bar shows the presence of very fine micropores, mostly present in interdendritic regions. Very rarely, shrinkage-type pores were observed. However, one macropore was always present in the fracture surface of all speciments. Variation in percentage elongation and 0.2% proof stress with volume percentage porosity showed that the elongation increased with porosity, whereas the 0.2% proof stress remained relatively unaffected. The data on UTS variation with porosity could not be assessed clearly.

They attempted to relate the pore area or pore length in a fracture to the ductility of the alloy. From their results, they conclude that the ductility and strength of the alloy depend mainly on the size of macropores rather than on the volume percentage of porosity, and that it is possible to estimate the ductility potential by knowing the size of the shrinkage cavity.

5. Hydrogen removal

The liabilities associated with the presence of hydrogen in Al/Al alloy melts have already been discussed above in detail, the influence of hydrogen on the mechanical properties (via the formation of gas porosity) being of particular concern. The need for thorough degassing of hydrogen from the melt thus becomes critical if the high strength levels of premier-quality castings are to be met. Consequently, foundrymen are faced with the problem of effectively reducing the gas content to acceptably low levels.

Several degassing methods have been developed for removing hydrogen; most of these methods employ "purging" techniques where an inert or reactive gas is bubbled through the melt. Argon or nitrogen or a mixture of either of these with chlorine or freon 12 are usually employed. The almost negligible partial pressure in the bubbles of the purging gas encourages the dissolved hydrogen to diffuse continuously into these bubbles, which rise and break out to atmosphere at the metal surface. The efficiency of the treatment depends upon the size/area of the bubbles, their speed, the purity of the gas and its method of introduction, as well as the furnace atmosphere and depth of the molten bath. The efficiency of the degassing is improved if the treatment uses very small bubbles that are well dispersed in the melt; by doing so the surface area is increased, diffusion distances are reduced and the contact time of the slower-rising smaller bubbles with the liquid metal is also extended [152].

The various degassing methods include simple techniques like tablet or lance degassing and others like gas fluxing and porous plug degassing [152], as well as more sophisticated but costly methods like the "spinning nozzle inert flotation" (SNIF) or the "fumeless in-line degassing" (FILD) processes [153, 154], dynamic vacuum treatment [155] and the more recent "rotary impeller degassing" (RID) technique that is fast gaining popularity [156]. The "foundry degassing unit" (FDU) and the "mobile degassing unit" (MDU) are modifications of the latter [157].

In addition to the purging techniques mentioned above, vacuum degassing is another alternative for hydrogen removal from the melt. Attempts to lower hydrogen content by creating a vacuum above the melt surface have been successful [158] and the theoretical basis for the same proven sound. Even partial vacua have been found to be effective, and developments and experience obtained with vacuum degass-

ing of aluminium are leading to an increasing use of this technology in foundries [159–161].

5.1. Kinetics and thermodynamics of hydrogen removal

Several methods exist for the removal of hydrogen from liquid metals. For Al/Al alloys, in particular, inert flush degassing and vacuum degassing constitute the two main treatment procedures. Gas flushing has long been known [162] and a number of studies have been reported on gas/inert gas flushing of melts [163–165]. Vacuum degassing is a relatively more recent procedure.

The design of a process involving either of these techniques is based on the mass transfer coefficient for hydrogen between the liquid metal and the gas phase (dilute in hydrogen). While the first theoretical studies in this context are those of Geller [166], who studied the equilibrium between purging gases and metal bath during flushing, Pehlke and Bement [167] are among the earliest workers to have presented a detailed and comprehensive account of the mass transfer of hydrogen between liquid aluminium and inert gas (argon) bubbles, and to give a quantitative evaluation of the mechanism of hydrogen removal. Other notable works in this area are that of Botor from Poland and those of the Norwegian group led by Engh, in collaboration with Sigworth. Botor [168, 169] has dealt with the kinetics of hydrogen degassing of molten aluminium by purge gases. Sigworth and Engh [170, 171] have examined in detail the chemical and kinetic factors as well as the thermodynamics related to hydrogen removal from aluminium. Engh and Pedersen [172] have proposed a model for hydrogen removal from molten aluminium by gas purging that includes various aspects of the phenomenon.

The theoretical aspects of hydrogen removal outlined below are broadly summarized from the above studies. For complete details, the reader is referred to the respective articles.

Under equilibrium conditions, the relationship between the dissolved gas that is removed and the flushing gas is given by

$$dN_g = dN_f\left(\frac{P_g}{P - P_g}\right) \quad (9)$$

where N_g and N_f are the volumes of dissolved and flushing gas, and P_g and P are the partial pressure of the dissolved gas in the bubble and the total pressure (in atm) on the system, respectively. In the case of hydrogen, the concentration of dissolved gas C_g is related to its equilibrium pressure in the bubble by Sieverts' law:

$$C_g = K_g P_g^{1/2} \quad (10)$$

K_g being a constant and C_g being expressed in wt %. Equations 1 and 2 combine to give

$$V_f = \frac{224}{M_g}\left[PK_g^2\left(\frac{1}{C} - \frac{1}{C_0}\right) + (C - C_0)\right] \quad (11)$$

which is the equation of Geller [166]. V_f is the volume of flushing gas in units of per kg of metal required to reduce the concentration of the dissolved gas (of molecular weight M_g) from C_0 to C.

Essentially, however, equilibrium between flushing gas and metal bath is reached only under the most ideal circumstances. In view of this, degassing is considered in terms of the processes which control the rate of approach to equilibrium.

Pehlke and Bement [167] attempted a quantitative evaluation of the mechanism of hydrogen removal from molten aluminium with argon. Based on their experimental results determined at 700 °C, they obtained a mass transfer coefficient of 3.9×10^{-2} cm s^{-1} for hydrogen removal from liquid aluminium, for bubbles of 0.4–1.0 cm diameter and a flow rate of 13.3 cm^3 s^{-1}, and derived a mathematical model for the same. Assuming mass transport control, and working through the various stages of the removal process, they obtained an expression for the instantaneous concentration C of the melt in terms of the original concentration C_0, the diffusion coefficient D of hydrogen dissolved in the liquid phase, the boundary layer thickness δ at the exposed melt surface (of area A_s), the mass transfer coefficient k_L for the rising bubbles, as well as several geometrical factors, given by

$$\ln\left(\frac{C}{C_0}\right) = -\left(\frac{DA_s}{\delta V_m} + \frac{3k_L F\tau_r}{r_b V_m}\right)t \quad (12)$$

τ_r being the time required for a bubble to rise through the melt, r_b the bubble radius, V_m the volume of the melt and F the flow rate of the flush gas, respectively, and where the thermal expansion of the bubbles as well as that caused by the reduced pressure head, the time of formation of the bubbles and the flow conditions were also taken into account.

The results of their experiments suggest that the removal of hydrogen from liquid aluminium by inert flush degassing is a non-equilibrium process controlled by mass transport in the liquid phase, and that the rate of removal is increased by increasing the flow rate and by decreasing the bubble size.

Further investigating the claims of Pehlke and Bement [167], Botor [169] carried out extensive studies of the kinetics of hydrogen desorption from molten aluminium using nitrogen, argon, chlorine and ($N_2 + Cl_2$) as the purge gases, and determined its dependence on the flow rate of the purge gas, the temperature and the geometry of the measuring system. He obtained and used the equation

$$k = \frac{G_m}{2F}\int_{X_H^e}^{X_H^b}\frac{1}{\Delta\pi}dX_H \quad (13)$$

to determine the experimental values of overall mass transfer coefficients of hydrogen in molten aluminium into the purge gas bubbles, k being the mass transfer coefficient, G_m the number of moles of metal examined (in Al moles), F the liquid metal–gas bubble interfacial area, $\Delta\pi$ the change of driving force of the process with change of liquid column and X_H the concentration of

hydrogen in aluminium (in H moles/Al moles), with the limits of X_H being from refining time $\tau = 0$ to its value at the metal level surface.

The theoretical value was estimated from the mass transfer coefficients β_c and β_g in the liquid and gaseous phases, respectively, to be

$$\frac{1}{k_i} = \frac{1}{2\beta_g} + \frac{n}{\beta_c} \quad (14)$$

n being an interchanging factor connecting the driving modulus in liquid and gaseous phases.

From his results Botor concludes that hydrogen desorption by gases is a diffusion process proceeding in non-equilibrium conditions and controlled by mass transfer of hydrogen in the liquid Al phase. The kind of purge gas used is not as critical as the method of its introduction into the melt. In other words, it is important to ensure that individual bubble flow is maintained, which can be adversely affected by high flow rates of the purge gas, leading to a decrease in the overall mass transfer coefficient. This value varies from 6.01×10^{-3} mol m^{-2} s^{-1} for nitrogen to 6.31×10^{-3} mol m^{-2} s^{-1} for argon to 8.39×10^{-3} mol m^{-2} s^{-2} for chlorine. It is found that hydrogen degassing of Al reaches its maximum value at a concentration of ~ 10 vol % of Cl_2 in N_2.

Sigworth and Engh [170] have obtained general relations for hydrogen removal rates when purging with inert gas or when using a vacuum. The complicated equation for hydrogen removal is shown by them to reduce to more simple expressions for certain values of a new dimensionless group, ψ/[pct H]. This "dimensionless hydrogen concentration" represents the ratio of the ability of hydrogen to diffuse to bubbles during their ascent to the capacity of the purge gas to remove hydrogen. From a consideration of the kinetic factors involved, and bearing in mind the series of steps in which hydrogen removal takes place, they obtain a relation of the form

$$\psi/[\text{pct H}] = \frac{JK^2}{2f_H^2[\text{pct H}]^2} = \frac{k\rho A p_{\text{inert}} K^2}{4f_H^2 100\, m_H G[\text{pct H}]} \quad (15)$$

directly related to the exit gas composition. (The symbols used in the above equation are defined in Sigworth and Engh [170]. The group

$$\frac{k\rho A\,[\text{pct H}]}{400\, m_H G}$$

gives the dimensionless ratio of the rate of hydrogen diffusion (in mol s^{-1}) to the rate of inert gas flow. The group

$$\frac{p_{\text{inert}} K^2}{f_H^2[\text{pct H}]^2}$$

gives the ratio of inert gas pressure to equilibrium hydrogen gas pressure. Their product forms the dimensionless hydrogen concentration ψ/[pct H]. ψ depends on the equilibrium constant, the mass transfer coefficient and the inert gas flow rate. When ψ/[pct H] ≤ 0.1, the process is rate-controlling. For values ≥ 1.0, the purge gas concentration is essentially at equilibrium with the melt and thermodynamic limitations apply. Vacuum treatment is seen to partially remove the equilibrium limitations found at atmospheric pressure.

The same authors have also presented an up-to-date review of the thermodynamic properties of Al alloys and have examined the thermodynamics involved under gas-purging and vacuum-treatment refining procedures, as well as the reaction of elements dissolved in Al alloys with reactive gases [171]. According to them, proper thermodynamic calculations are essential in the selection of a suitable refining experiment. Calculated "interaction coefficients" for various elements in liquid Al binary alloys are also presented.

5.2. Methods of hydrogen removal

The various methods that have been developed over the years for the removal of hydrogen are summarized in Table I [157]. With the exception of vacuum degassing, all the other techniques are purging ones and involve the passing of an inert or active gas through the melt. As the stream of gas bubbles passes through the melt, the hydrogen in the liquid metal diffuses into these bubbles and is removed to the atmosphere when

TABLE I Review of degassing systems (after Pattle [157])

System	Treatment gas	Efficiency of H_2 removal	Fume evolution	Degassing rate	Capital cost	Operator involvement
Tablets	Reactive	High	High	Moderate	None	High
	Inert	Moderate	None	Moderate	None	High
Lance	Reactive	High	High	Moderate	Low	Moderate
	Mixed	Moderate	Moderate	Low	Low	Moderate
	Inert	Low	None	Low	Low	Moderate
Rotary devices	Mixed	High	Moderate	High	Moderate	Low
	Inert	High	None	High	Moderate	Low
Vacuum	None	High	None	Low	High	Low

the bubbles break at the surface of the melt. Reactive gases (e.g. chlorine or freon) work more effectively than inert gases (e.g. nitrogen or argon) due to the chemical reactions that result when such gases are introduced into the metal, and the rate of removal is therefore greater. However, fume evolution is a major environmental problem, so gas mixtures are used instead, which contain less than 10% chlorine, example Trigas [173]. With nitrogen, however, the degassing efficiency is much lower and there is the possibility for the formation of nitride inclusions [174].

The methods used for these purging systems can involve tablets containing hexachloroethane which are plunged into the melt and held therein, where they decompose to provide a supply of degassing bubbles, or they can be simple lances carrying gas from a cylinder or supply in the foundry.

The tablet method does not require the equipment necessary when using a gas, and on account of its simplicity is used more extensively. Degassing results can be inconsistent, however.

With lance degassing, equipment for the storage, monitored distribution and pressure regulation of the gas is required. The bubbles produced are usually large in size and can cause oxidation and turbulence at the melt surface. To avoid increase in gas pick-up, the degassing is done when the melt temperature is falling, and the process takes typically 15–20 min for 50 kg melts.

In comparatively small foundries, where Al alloy castings are produced by pressure die casting, the melt refining is often carried out using hexachloroethane tablets or else preferably by injection with argon or nitrogen. The important part of such a refining system is the gas-distributing lance. In the USSR, titanium tubes are preferred to graphite ones for lances. However, they can be expensive to produce. Zolotoi *et al.* [175] have proposed a simple refining unit for industrial use that employs a lance of novel design, fabricated from carbon-steel water or gas piping and wrapped in glass-fibre fabric (aluminoborosilicate glass). The lance has been tested in gas-fired furnaces with graphite–chamotte crucibles that produce 150 kg of AL2 aluminium alloy per cycle. Comparative trials with such glass-fibre fabric-wrapped lances have shown that the H_2 gas content is reduced by 25–30%. The glass fibres remain strong even at melt temperatures and the lances can withstand up to 25 or more refining cycles. The refining gases used are super grade argon or nitrogen. With a flow rate of 5 l min^{-1}, the treatment time takes about 15 min for a 150 kg melt load. Commercial trials have shown that argon lancing greatly improves the properties of the castings, especially the ductility. According to Zolotoi *et al.*, the use of argon lancing has also lowered production costs by about 220 roubles per tonne of castings.

Although the use of chlorine gas fluxing has proved highly satisfactory in terms of efficiency and cost, the toxic effects of chlorine fumes and associated pollution problems severely restrict its use in degassing. Consequently, other gas mixtures have been tried that utilize inert gases with or without chlorine. There is, however, a loss of degassing potential [176–178].

The development of a degassing process combining the efficiency of chlorine with the non-polluting properties of inert gases was first achieved by Dore *et al.* [176], for cast shop use with an inert gas–freon 12 combination. Tests were conducted to establish the degassing rates of various gases including Cl_2, N_2, N_2–CO–Cl_2 and (N_2 + freon 12) mixtures. The degassing curves for these are shown in Fig. 16, where the (N_2–5% freon 12) mixture is seen to approach the degassing efficiency of Cl_2 gas. It was also demonstrated by these authors that the efficiency could be further enhanced by using a molten salt flux cover in addition to the inert gas–freon 12. NaCl–KCl + fluoride salt or $MgCl_2$ + KCl fluxes were found suitable for Al alloys containing less than or more than 1% Mg, respectively. The process, patented by Consolidated Aluminium Corporation, St Louis, Missouri [179], was further tested on A356 and A201 alloy melts, the results of which are shown in Fig. 17a and b. Fig. 18 depicts the schematic diagram of the inert gas–freon 12 gas distribution system [180].

The shortcomings of the tablet and lance methods apparently left room for much improvement, and porous plug degassing was evaluated in this respect, the advantage being that it would lead to the formation of very small bubbles that would increase the degassing efficiency (as outlined earlier). An extensive research programme, conducted at Loughborough University, UK, evaluated porous plug degassing of aluminium alloys with the aim of determining the most suitable material for the manufacture of porous plugs as well as the efficiency of such a system.

Water simulation studies of several porous plug configurations were carried out by Booth and Clegg [152] to determine the effects of plug porosity and the flow rate and pressure of the gas on the bubble size, density and distribution. Hockey stick-, end-, sandwich-, hemispherical- and tapered-type porous plugs were studied, employing both vertical and U-tube lances. Materials used included silicon carbide, molochite, alumina, mullite, zircon and graphite. Flow patterns for the different configurations were also es-

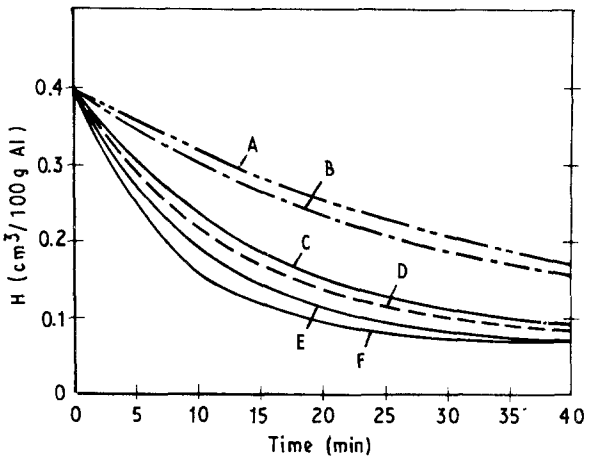

Figure 16 Influence of fluxing gas on degassing rate of 99.85% pure aluminium [176]: (A) N_2, (B) N_2–10% CO–10% Cl_2, (C) N_2–5% freon 12, (D) Cl_2, (E) N_2–10% and 20% freon 12, (F) N_2–25% freon 12; 2045 kg melt, melt temperature 720 °C, gas flow 90 l min^{-1}.

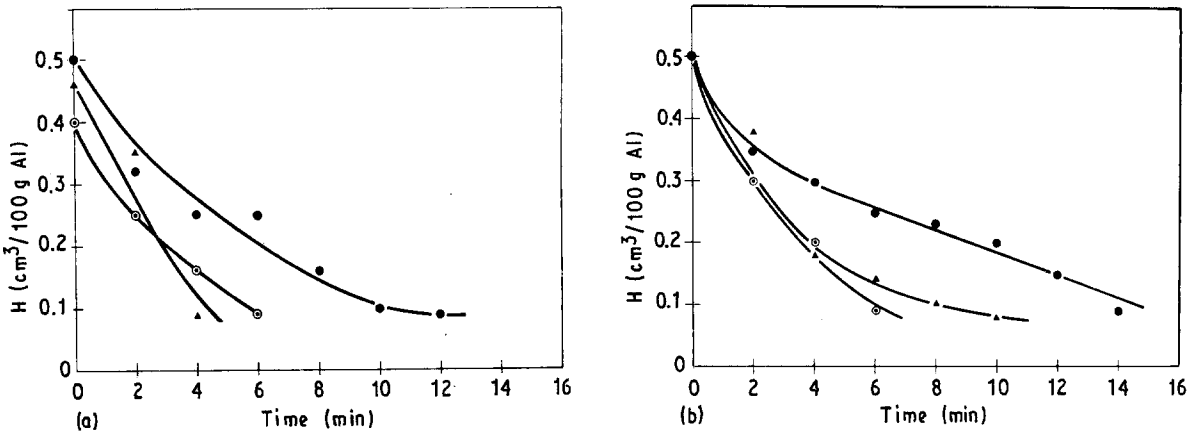

Figure 17 Influence of fluxing gas on degassing rate of 60 kg melts of (a) A201 alloy (melt temperature 790 °C) and (b) A356 alloy (melt temperature 730 °C) [180]: (▲) N_2–5% freon 12, (●) N_2, (⊙) Cl_2. Gas flow 6 l min^{-1}.

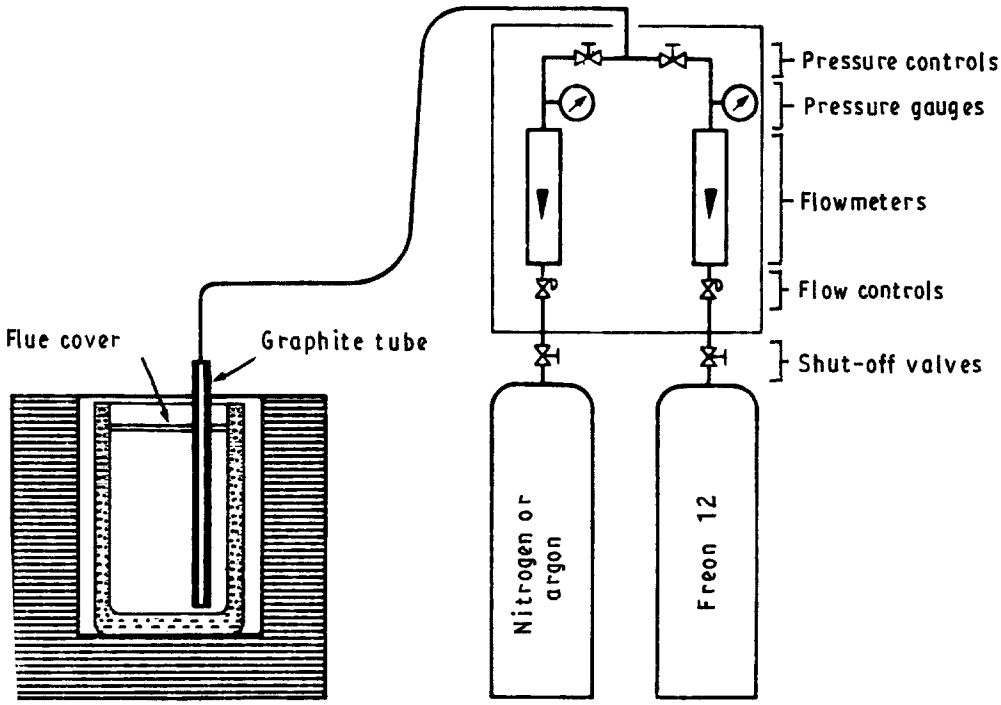

Figure 18 Schematic diagram of inert gas–freon 12 gas distribution system [180].

tablished. The tests carried out in a water bath revealed that all porous plug configurations were more effective than the lances in reducing bubble size and increasing bubble density and distribution. The most effective configuration was that of the hockey stick; however, the tapered plug (attached to the base of a clay–graphite, sheathed steel lance) proved to be more practical. Also, the porous plugs produced a more definite flow pattern than the degassing lances.

From their studies, Booth and Clegg concluded that alumina and silicon carbide are the most suitable materials for porous plugs, whereas porous graphite is unsuitable. The bubble size, density and distribution increases with increasing gas flow rate, increasing the degassing efficiency. Strangely enough, the use of a nitrogen–5% freon gas mixture did not provide improvements in the efficiency as expected. Plane faces directed at the base of the melt are to be avoided when designing the porous plug, as the bubbles from such faces tend to coalesce. Overall, porous plug degassing is found to be more efficient. Fig. 19 compares the porous plug and lance degassing results obtained by these authors.

Dividing the treatment gas into very small bubbles as well as dispersing them throughout the liquid melt should result in further improving the degassing efficiency. These effects can be achieved by using rotary devices. Dating from the work of Szekely [181] in this area (originating with a device in the form of a graphite flotation cell that was immersed in aluminium for purification purposes), various degassing equipment have been developed, using rotary impeller devices patented by different workers [156, 182, 183].

Results of the study and modelling of the degassing process by the Norwegian group of Engh and coworkers together with Sigworth led to the development of a new rotary impeller head design and subsequently the rotary impeller degassing [RID] process. The primary advantage of RID is more rapid degassing. Commercially, it has been found that an

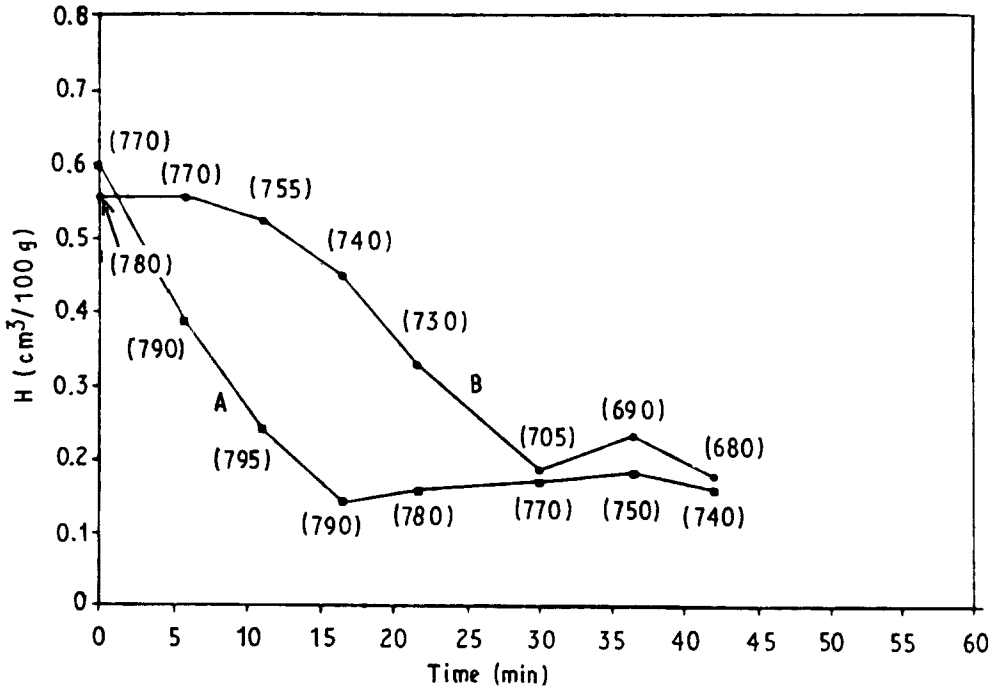

Figure 19 A comparison between (A) porous plug and (B) lance degassing (the figures in parentheses indicate temperature) [152].

RID unit degasses in about one-half to one-third the time required by tablets, lances or porous plugs. It is also capable of reaching lower gas levels.

A typical RID degassing equipment consists of an insulated steel cover sized to fit over standard crucibles, and which supports an air motor and a high-temperature sealed bearing unit placed just off centre. The shaft and impeller are suspended from the bearing unit. The latter transfers the purge gas through a graphite lance to the impeller head. A control panel transports compressed plant air and purge gas to the impeller unit through rubber hoses using standard pipe fittings. The panel supplies a converted voltage of 24 V for instrumentation [184].

The key to the whole process is the rotary head's ability to break the normally large bubbles into very small ones, thereby significantly increasing the surface area of available purge gas and, therefore, the efficiency. Distributing these bubbles by stirring further improves the degassing. The impeller head constitutes the most important part of the unit. Its shape and speed of rotation break the purge gas up into fine bubbles and distribute it throughout the melt. The diameter and shape of the impeller head are determined by the size of the crucible. The cover on the unit is also of importance as a correctly sized cover helps to reduce heat loss and maintain an inert atmosphere above the melt.

According to Anderson [184], trial runs with an RID unit conducted at Hitchcock Industries, Bloomington, Minnesota, proved satisfactory. The degassing was found to be three times more effective than the standard lance degassing techniques being employed by them at the time. The trials were performed on 1100 lb (499 kg) melts of A357 alloy. Two problems were initially encountered: the very short life of the graphite impeller shafts due to oxidation at the metal line, and a loss of degassing efficiency. Both were corrected by using oxide retardant-treated graphite material for the shaft and adding a purge valve to the unit.

Fig. 20a shows a diagram of the new rotary impeller degassing unit designed at Reading Foundry Products, Pennsylvania by Sigworth *et al.* [156], where part A contains an air-cooled motor assembly, part B is a 0.25 in. (6 mm) thick steel plate lid assembly with a 2 in. (51 mm) thick refractory lining, and parts C and D are the impeller shaft and head, respectively. Fig. 20b shows an actual RID unit in motion. The method was tested versus porous plug and lance techniques for a 500 lb (227 kg) melt of 356 Al alloy. The results are shown in Fig. 21. The lance was ineffective, and while the porous plug worked reasonably well, the rotary impeller was the quickest and most efficient.

Based on its performance, rotary impeller degassing has found rapid acceptance in the foundry. Foseco International of Birmingham, UK have developed the "foundry degassing unit" (FDU), which uses a unique patented rotor design that is capable of degassing a 250 kg ladle of Al alloy in 3–5 min using nitrogen or a mixed gas system. A subsidiary model of the FDU, the "mobile degassing unit" (MDU), developed by BNF Metals Technology Centre, is a small and portable rotary degassing unit, designed for mobility around the foundry and suitable for treating smaller (100–200 kg) furnaces. Foseco International is likewise responsible for the exclusive manufacture and marketing of this unit.

In the FDU unit, the great number of small bubbles of the purging gas required for hydrogen removal is achieved by means of a unique rotor design which facilitates thorough mixing of gas and metal at the point of gas introduction. From test trials, a rotation speed of 450 r.p.m. and gas flow of $10\,l\,min^{-1}$ were found to be the optimum operating conditions for 250 kg of metal. Using a 200 mm diameter rotor, the

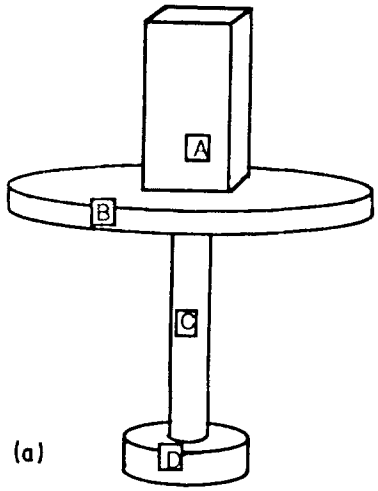

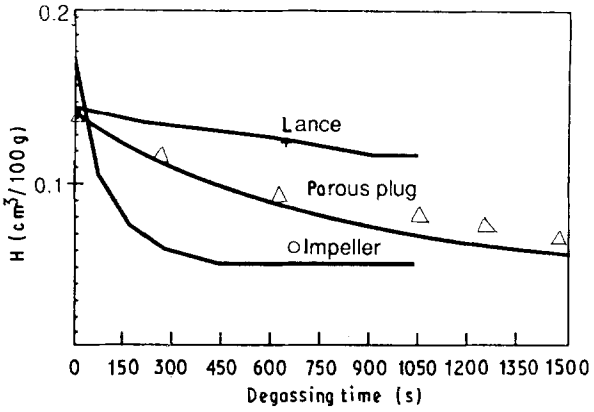

Figure 21 Results obtained with lance, porous plug and rotary impeller degassing techniques in a 500 lb (227 kg) melt [156].

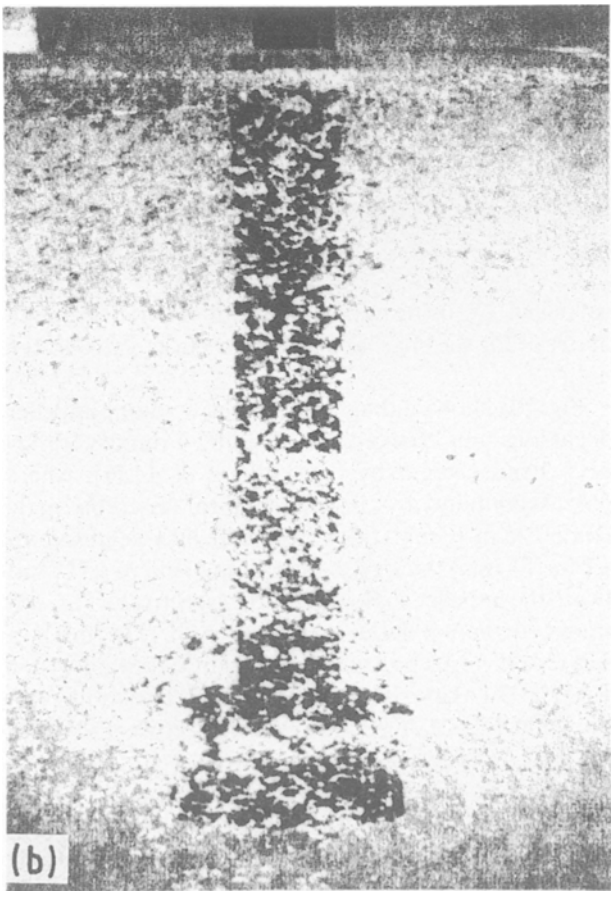

Figure 20 (a) Schematic diagram of rotary impeller degassing unit [156]; (b). Actual rotary impeller head shown in motion. Note the small bubble size and wide bubble dispersion.

hydrogen content of 250 kg of aluminium could be reduced from 0.39 p.p.m. to an average of 0.15 p.p.m. in 5 min [157]. The production FDU system is equipped with pre-set functions of rotor speed, gas flow and treatment time. All that is required of an operator is to bring the ladle to the FDU and start it operating. At the end of the treatment time, the unit indicates that the treatment is over.

The MDU is essentially a portable model of the FDU. The production unit consists of a small trolley which carries a gas bottle and drive and handling system for the graphite rotor. Of simple robust design, this rotor has proved to be efficient when tested in a wide variety of alloys (LM4, 6, 10, 11, 13, 16, 25, L99, L119), under widely varying foundry conditions. Treatment times of 5 min with a nitrogen flow rate of 5–7 l min^{-1} generally reduced the hydrogen content to below 0.1 cm^3 per 100 g [157].

In addition to the high degassing rates and low residual gas levels obtained by these units, there is no environmental pollution or operator error.

At Aluminium Pechiney, France, hydrogen and oxide removal of aluminium alloys in the foundry is carried out using the Alpur system of treatment developed by them [183]. The Alpur treatment, aimed at producing "quality metal", utilizes a rotating agitator that is placed in the middle of a tilting ladle installed between the furnace and the pouring stage. The metal within the ladle is treated by the rotating agitator. The agitator, patented as "Alpur", consists of a rotor made from suitable graphite material. It allows for an intimate contact between the gas and the metal in the interior of the rotor, and the distribution and dispersion of very fine bubbles throughout the molten metal. The agitator rotates with an average speed of 150–200 r.p.m. The simple design of the agitator allows for its easy maintenance and replacement.

In 1986 a new automated flux injection system was introduced to the United States aluminium casting industry. The technology for this process existed in Europe and gained acceptance in various foundries producing sand, permanent-mould and die castings [185]. The flux injection process for aluminium treatment eliminates hydrogen as well as oxides. In view of the faster treatment times, improved fluidity, consistent quality of the cast, cleaner working environments and lower processing costs, this technology is now considered by many of its users to be the ultimate state-of-the-art method of hydrogen gas removal and that of oxide elimination from an aluminium alloy melt. Together with gas and oxide removal, the process can be used at the same time to modify and refine the alloys being treated, thus saving treatment time. Hepworth Minerals and Chemicals (HMC) developed the initial flux injection technology in the early 1980s and have been continuously updating the process. This has led to the development of maintenance-free machines that are easy to operate [186].

Fig. 22 shows a schematic diagram of the HMC flux injection process equipment. Flux is fed into the mixing chamber through a calibrated rotary feed, then mixed with nitrogen gas which acts as a carrier for the

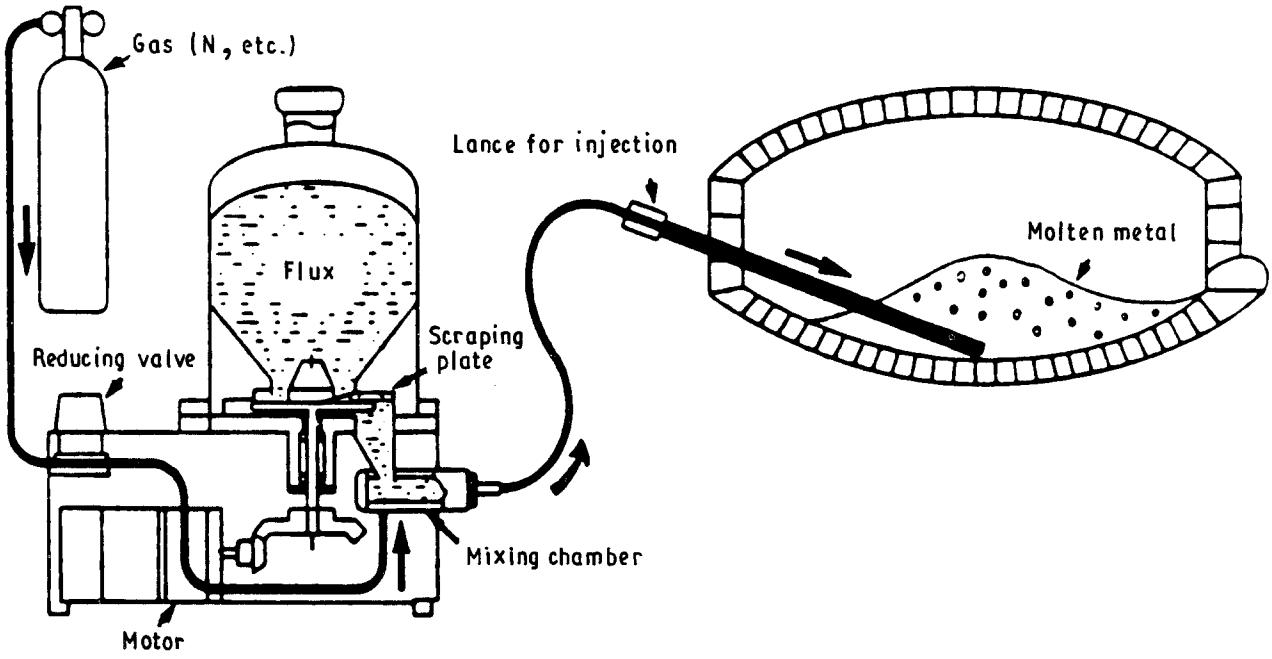

Figure 22 The HMC flux injection process equipment. After Harriss [186].

flux and is introduced below the surface of the melt using a ceramic-coated lance. The chemical and mechanical reactions generated ensure that the effect of the flux is almost totally efficient and, consequently, so is the hydrogen removal. A typical metal treatment for a wide range of alloys would be 0.2% of Fesflux NF 20/4 injected into the metal for 5–10 min. 5 min of treatment time brings down the hydrogen level from 0.35 to about 0.08 cm^3 per 100 g. A further 5–10 min standing time will allow the level to reach 0.05–0.06 cm^3 per 100 g.

The flux injection system has shown itself to be a viable, cost-effective method for treating molten aluminium with consistent high-quality end-product resuts.

Yet another system used in the degassing of molten aluminium is the "degassing Multicast™ filtration system", a combined degassing and filtration unit proposed by Metaullics. The Metaullics degassing Multicast system (DMC) provides excellent degassing efficiency coupled with rigid media, bonded particle filtration in the Multicast configuration [187].

The DMC unit consists of a heated box with separate chambers for degassing and filtration. A gas-fired flat-flame radiant heat burner with an adequate heat supply for melting and holding of the molten metal is normally employed as the heat source. The degassing chamber utilizes a special design of porous plug (Narco Al Clean), which provides a fine bubble size and good mixing in the chamber. The porous plugs are used on the floor of the degassing chamber to introduce the fluxing gas and to allow for the maximum possible time of the bubbles in the bath as well as good mixing in the chamber. The filtration chamber contains a Metaullics Multicast filter assembly. Inlet and outlet designs may vary, each unit being customized to meet individual casting configurations. Based upon the specified operating and environmental/working conditions, the degassing chamber of the DMC unit is accordingly designed by Metaullics to blend in with the filter requirements. With the DMC system, effective removal of hydrogen to levels ≤ 0.10 cm^3 per 100 g Al have been achieved, the hydrogen level reduction being somewhat dependent on flow rate. Although initially applied for continuous casting operations, it is expected that the technology will be extended to DC casting as well.

5.3. Vacuum degassing

Attempts to decrease hydrogen levels by creating a vacuum above the melt surface have been shown to be successful [158]. It has been the experience that even partial vacua are adequate under suitable conditions [160].

In vacuum-accelerated degassing the escaping hydrogen is able to break the oxide films on the surface, which otherwise normally prevent its escape [159]. As gas bubbles are not admitted to the melt, it becomes important to stir the metal throughly, since degassing can now only occur at the surface. The hydrogen removal takes place in a series of three steps: (i) by diffusion from the immediate metal surface that is continually being renewed by convection, (ii) by free evaporation at the surface, and (iii) by diffusion through the gas phase [170]. The overall effective mass transfer coefficient can be calculated from the individual coefficients for each of the three steps:

$$k_e = \left(\frac{1}{k_1} + \frac{1}{k_2} + \frac{1}{k_3}\right) - 1$$

As the diffusion rate, solubility and other material characteristics put an optimum level to the degassing efficiency, and entail longer times in spite of the vacuum, the process requires to be accelerated. This is done by means of a scavenging gas introduced at the bottom of the melt [188, 189]. In the case of gas-stirred baths, because of the partial pressure decrease

in the bubbles rising to the evacuated surface, the bubble size increases, resulting in a slight decrease in the mass transfer coefficient. That is to say, the bubble size becomes a function of height, unlike the case of atmospheric degassing. With gas-stirred vacuum degassing, the consumption of the purge gas is considerably reduced (up to seven times, even), since the equilibrium constraints associated with atmospheric degassing are removed.

Although vacuum degassing has not yet been widely adopted by the aluminium foundry on account of the high costs involved, increasing numbers of workers have been investigating this system of degassing as evidenced by the literature.

Russian workers [190] have reported a breakthrough in vacuum degassing technology of aluminium, in which molten metal is transferred to the vacuum degassing furnace in the form of a jet and *in situ* degassing is effected. The turbulence caused by the melt jet produces greater efficiency as well as considerable reduction of the degassing time [190]. The process has been commercially tested and H_2 levels of 0.02, 0.12 and 0.10 cm^3 per 100 g have been reported for Al–Mg2, Al–Mg5 and Al, respectively. Compared to traditional degassing, this process enabled a 30–80% increase of melter–caster output.

Hilgenfeldt and Hilpmann [191] have conducted tests on Al–Si alloys (G–AlSi10Mg, G–AlSi7Cul) and have shown that the hydrogen content can be reduced by approximately 50% by vacuum treatment without impairing the refinement through Na loss [191]. The dependence of the vacuum degassing on temperature and treatment time was also studied, where the gas porosity was found to decrease with increasing treatment time as well as with a decrease in the melt temperature. A scavenging effect with respect to nonmetallic inclusions was also found to occur.

Sivaramakrishnan and Mahanti [159] at the National Metallurgical Laboratory, India have reviewed various methods of aluminium degassing and have shown that degassing of Al alloy melts can be successfully carried out with nitrogen under partial vacuum, and that there is a tendency for modification under these conditions of degassing.

Schaefers *et al.* [160] have considered degassing in a partial vacuum as a new purification method for Al melts. According to them, environmental compatibility of a method is as important as process efficiency and application simplicity, and treatment of molten aluminium in a partial vacuum combines all these features. In the method proposed by them, the melt is contained in a crucible made of porous material, e.g. SiC or graphite–clay. On applying the vacuum, air/furnace exhaust gases penetrate the pores and rise in a steady stream of fine bubbles through the melt to its surface. Effective removal of hydrogen and floating oxide particles could be demonstrated on various Al alloys (Al–Si, Al–Si–Mg, Al–Si–Cu, Al–Cu–Ti and Al–Cu–Ni–Co–Sb–Zr). A 10 min vacuum treatment was sufficient to give high-quality grades with improved mechanical properties.

Recently, Choudhury and Lorke [161] have reviewed the developments and practical experience in areas of vacuum degassing of aluminium and believe that these developments are leading to the increasing use of this technology in foundries. According to them, vacuum degassing is an effective way of removing dissolved gases, oxides and other impurities. The mechanical strength of vacuum-degassed castings is greater than that of chlorine-degassed ones. Fig. 23 compares the mechanical properties of vacuum- and chlorine-degassed Al test pieces [192], while Fig. 24 is a photograph of cast specimens before and after vacuum degassing [193]. Similar pictures have also been shown by Hilgenfeldt and Hilpmann [191] for Si 710 alloy in their work on the vacuum treatment of aluminium melts.

The use of suitable vacuum technology produces, in addition, results that are independent of atmospheric effects, starting material and pretreatment. Vacuum degassing, unlike chlorine degassing, can be integrated safely into production lines. Although in principle there are two types of vacuum treatment plant, namely the chamber version [161] and the hood version [193], the demands made on plant design would be based on the current needs of the foundry and on future metallurgical and economic conditions.

6. Summary

Various aspects relating to the development of premium-quality aluminium alloy castings have been reviewed. Achievement of such castings is mainly obtained through careful control of the hydrogen level in

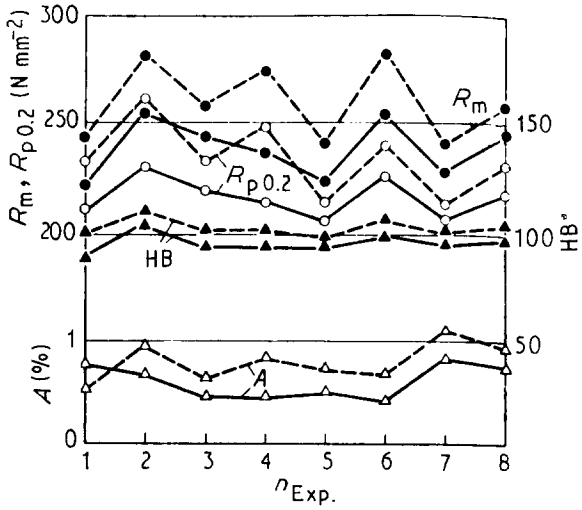

Figure 23 Mechanical properties of (– – –) vacuum- and (——) chlorine-degassed Al test pieces. After Curavic [192].

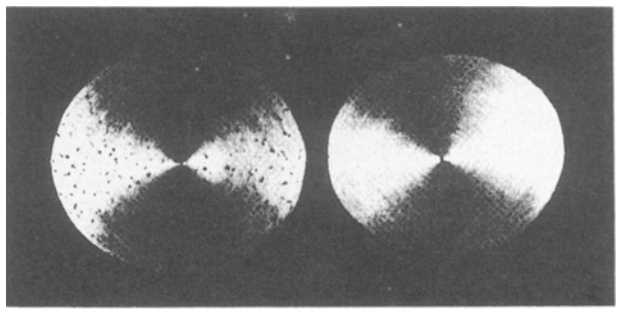

Figure 24 Cast specimens before (left) and after (right) vacuum degassing [193].

the molten metal prior to casting. Methods of hydrogen measurement and degassing have been reviewed in detail, covering various methods in both areas to date.

Problems arising from hydrogen-related gas porosity/microporosity have been addressed, as well as the effects of modification on both hydrogen pick-up and porosity. The effect of porosity on the mechanical properties of such castings has also been discussed.

Acknowledgements

The authors acknowledge the financial support received from the Natural Sciences and Engineering Research Council of Canada, the Fondation Sagamie de l'Université du Québec à Chicoutimi and the Société d'électrolyse et de chimie Alcan (SECAL).

References

1. D. E. J. TALBOT, *Int. Metall. Rev.* **20** (1975) 166.
2. F. O. TRAENKNER, *Modern Casting* (1981) 44.
3. E. F. EMLEY and P. A. FISHER, *J. Inst. Met.* **85** (1956–57) 236.
4. W. BAUKLOH and F. OESTERLEN, *Z. Metallkde* **30** (1938) 386.
5. M. B. BEVER and C. F. FLOE, *Trans. AIME* **156** (1944) 149.
6. C. E. RANSLEY and H. NEUFELD, *J. Inst. Met.* **74** (1948) 599.
7. W. R. OPIE and N. J. GRANT, *Trans. AIME* **188** (1950) 1237.
8. J. KOENEMAN and A. G. METCALFE, *Trans. ASM* **51** (1959) 1072.
9. C. L. THOMAS, *Trans. AIME* **239** (1967) 485.
10. W. EICHENAUER, K. HATENBACH and A. PEBLER, *Z. Metallkde* **52** (1961) 684.
11. W. EICHENAUER, *ibid.* **59** (1968) 613.
12. F. G. JONES and R. D. PEHLKE, *Met. Trans.* **2** (1971) 2655.
13. D. E. J. TALBOT and P. N. ANYALEBECHI, *Mater. Sci. Technol.* **4** (1988) 1.
14. J. CZOCHRALSKI, *Z. Metallkde* **14** (1922) 227.
15. K. IWASÉ, *Sci. Rep. Tôhoku Imp. Univer.* **15** (1926) 531.
16. P. RÖNTGEN and H. BRAUN, *Metallwirtschaft* **11** (1932) 459.
17. P. RÖNTGEN and F. MÖLLER, *ibid.* **13** (1934) 81.
18. L. L. BIRCUMSHAW, *Trans. Faraday Soc.* **31** (1935) 1439.
19. H. WINTERHAGER, *Alum. Arch.* **12** (1938) 7.
20. W. BAUKLOH and M. REDJALI, *Metallwirtschaft* **21** (1942) 683.
21. A. SIEVERTS, *Z. Metallkde* **21** (1929) 37.
22. C. E. RANSLEY, D. E. J. TALBOT and H. C. BARLOW, *J. Inst. Met.* **86** (1957–58) 212.
23. C. E. RANSLEY and D. E. J. TALBOT, *ibid.* **84** (1955–56) 445.
24. P. D. HESS, *J. Met.* **25** (1973) 46.
25. W. EICHENAUER and A. PEBLER, *Z. Metallkde* **48** (1957) 373.
26. C. E. RANSLEY and D. E. J. TALBOT, *ibid.* **46** (1955) 328.
27. R. EBORALL and C. E. RANSLEY, *J. Inst. Met.* **71** (1945) 525.
28. K. E. HONER and Z. YOULING, *Giessereiforschung* **39** (1987) 34.
29. R. Y. LIN and M. HOCH, *Met. Trans. A* **20A** (1989) 1785.
30. M. HOCH and I. ARPSHOFEN, *Z. Metallkde* **75** (1984) 23.
31. J. R. DENTON and J. A. SPITTLE, *Mater. Sci. Technol.* **1** (1985) 305.
32. S. JACOB, *Fonderie* **363** (1977) 13.
33. J. CHARBONNIER, J. J. PERRIER and R. PORTALIER, *AFS Int. Cast. Met. J.* **3** (1978) 87.
34. Y. KOYA, *Imono (J. Jpn. Foundrymen's Soc.)* **52** (1980) 558.
35. B. CLOSSET and J. E. GRUZLESKI, *AFS Trans.* **89** (1981) 801.
36. P. D. HESS and E. V. BLACKMUN, *ibid.* **83** (1975) 87.
37. K. ALKER and V. HIELSCHER, *Aluminium* **48** (1972) 362.
38. K. E. HONER, *Giessereiforschung* **34** (1982) 1.
39. B. CLOSSET and J. E. GRUZLESKI, *Met. Trans. A* **13A** (1982) 945.
40. S. M. D. GLENISTER and R. ELLIOTT, *Met. Sci* **15** (1981) 181.
41. J. GORBRECHT, *Giesserei* **65** (1978) 158.
42. P. C. BORBE *et al.*, *ibid.* **69** (1982) 393.
43. P. DAVAMI and M. GHAFELEHBASHI, *Br. Foundryman* **72** (1979) 4.
44. J. E. GRUZLESKI, Proceedings of the 2nd International Conference on Molten Aluminium Processing, Orlando; Florida, November 6–7, 1989, American Foundrymen's Society, Dés Plaines, Illinois (1989) p. 1–1.
45. F. C. DIMAYUGA, N. HANDIAK and J. E. GRUZLESKI, *AFS Trans.* (1988) 83.
46. H. SHAHANI, *Scand. J. Metall.* **14** (1985) 306.
47. S. YANEVA, N. STOICHEV and L. STOYANOVA, *Tekh. Misul.* **26** (1989) 103.
48. M. HASHEMI-AHMADY, *Diss. Abst. Int.* **49** (1989) 367.
49. N. TENEKEDJIEV, D. ARGO and J. E. GRUZLESKI, *AFS Trans.* **97** (1989) 127.
50. G. K. SIGWORTH, *ibid.* **95** (1987) 303.
51. W. EICHENAUEUR and J. MARKOPOULOS, *Z. Metallkde* **65** (1974) 649.
52. C. J. SMITHELLS, "Metals Reference Book", 5th Edn (Butterworths, London, 1975).
53. M. MOKARAM, PhD Thesis, Brunel University, London (1976).
54. L. M. FOSTER, *et al.*, *Nucleonics* **21** (1963) 53.
55. J. O'. M. BOKRIS and P. K. SUBRAMANYAN, *J. Electrochem. Soc.* **118** (1971) 1114.
56. J. F. NEWMAN and L. L. SHREIR, *Corros. Sci.* **11** (1971) 25.
57. F. R. COE and J. MORETON, *J. Iron Steel Inst.* **204** (1966) 366.
58. F. De KAZINCZY, *Acta Metall.* **7** (1959) 525.
59. R. A. ORIANI, *ibid.* **18** (1970) 147.
60. T. BONISZEWKI and J. MORETON, *Br. Weld. J.* **14** (1967) 321.
61. M. L. HILL and E. W. JOHNSON, *Trans. AIME* **221** (1961) 622.
62. T. ISHIKAWA and R.B.McLELLAN, *Acta Metall.* **34** (1986) 1091.
63. C. E. RANSLEY and D. E. J. TALBOT, *J. Inst. Met.* **88** (1959–60) 150.
64. J. E. HARRIS and P. G. PARTRIDGE, *ibid.* **93** (1964–65) 15.
65. B. CHEW, *Met. Sci. J.* **5** (1971) 195.
66. D. E. J. TALBOT and D. A. GRANGER, *J. Inst. Met.* **92** (1963–64) 290.
67. K. J. BRONDYKE and P. D. HESS, *Trans. Met. Soc. AIME* **230** (1964) 1542.
68. S. A. LEVY, *AFS Trans.* **93** (1985) 889.
69. W. HUFNAGEL, *Aluminium* **59** (1983) 266.
70. J. E. GRUZLESKI, N. HANDIAK, H. CAMPBELL and B. CLOSSET, *AFS Trans.* **94** (1986) 147.
71. J. P. MARTIN, F. TREMBLAY and G. DUBÉ, *Light Metals* (1989) 903.
72. D. A. ANDERSON, D. A. GRANGER and R. R. AVERY, *ibid.* (1990) 769.
73. J. A. ROGERS, *Foundry Trade J.* **151** (1981) 3216.
74. W. D. LAMB, *Light Metals* (1984) 1345.
75. F. DEGRÉVE and C. JARDIN, *Met. Trans. B* **6B** (1975) 545.
76. F. DEGRÉVE, *J. Met.* (1975) 21.
77. R. D. PEHLKE, Foundry Processes: Their Chemistry and Physics, G. Katz and C. F. Landefeld (eds) General Motors Research Laboratories, Warren, Michigan, September 1986 (Plenum Press, New York, 1988) pp. 427–445.
78. Q. T. FANG, P. N. ANYALEBECHI and D. A. GRANGER, *Light Metals* (1988) 977.
79. D. E. J. TALBOT and D. A. GRANGER, *J. Inst. Met.* **92** (1963–64) 290.
80. R. L. COBLE and M. C. FLEMINGS, *Met. Trans. A* **2A** (1971) 409.
81. H. FREDRIKSSON and I. SVENSSON, *Met. Trans. B* **7B** (1976) 599.

82. P. M. THOMAS and J. E. GRUZLESKI, *ibid.* **9B** (1978) 139.
83. S. N. TIWARI and J. BEECH, *Met. Sci.* **12** (1978) 356.
84. J. E. GRUZLESKI, P. M. THOMAS and R. A. ENTWHISTLE, *Br. Foundryman* **71** (1978) 69.
85. F. WEINBERG and D. A. HIRSCHFELD, *Met. Sci.* **13** (1979) 335.
86. M. ABBAS, G. R. ST-PIERRE and C. E. MOBLEY, *AFS Trans.* **94** (1986) 47.
87. T. S. PIWONKA and M. C. FLEMINGS, *Trans. Met. Soc. AIME* **236** (1966) 1157.
88. J. CAMPBELL, *Cast Met. Res. J.* **4** (1969) 1.
89. *Idem, Trans. Met. Soc. AIME* **239** (1967) 138.
90. *Idem,* "The Solidification of Metals", Publication 110 (Iron and Steel Institute, London, 1967) p. 18.
91. K. KUBO and R. D. PEHLKE, *Met. Trans. B.* **16B** (1985) 359.
92. H. FREDRIKSSON, *ibid.* **7B** (1976) 599.
93. D. ARGO and J. E. GRUZLESKI, *AFS Trans.* **96** (1988) 65.
94. Q. T. FANG and D. A. GRANGER, *ibid.* **97** (1989) 989.
95. D. R. POIRIER, K. YEUM and A. L. MAPLES, *Met. Trans. A.* **18A** (1987) 1979.
96. K. MURAKAMI, C. Y. LIU and T. OKAMOTO, in "Solidification Processing", edited by J. Beech and H. Jones (Institute of Metals, London, 1988) p. 454.
97. Q. T. FANG and D. A. GRANGER, *Light Metals,* (1989) 927.
98. M. F. JORDAN, *et al., J. Inst. Met.* **91** (1962–63) 48.
99. K. OHSASA, T. OHSHIMA and T. TAKAHASHI, *J. Jpn. Inst. Light Met.* **39** (1989) 109.
100. K. KUBO and R. D. PEHLKE, *AFS Trans.* **94** (1986) 753.
101. J. ZOU, K. TYNELIUS, S. SHIVKUMAR and D. APELIAN, in "Production, Refining, Fabrication and Recyling of Light Metals", edited by M. Bouchard and P. Tremblay, (Pergamon, New York, 1990) p. 323.
102. B. R. DEORAS and V. KONDIC, *Foundry Trade J.* **100** (1956) 361.
103. R. ENTWHISTLE, J. E. GRUZLESKI and P. M. THOMAS, in Proceedings of Conference on Solidification and Casting of Metals, University of Sheffield, July 1977 (The Metals Society, London, 1977) p. 345.
104. A. A. KHOMITSKII, *Liteinoe Proizvodstvo* No. 7 (1988) 11.
105. T. J. HURLEU and R. G. ATKINSON, *AFS Trans.* **93** (1985) 291.
106. B. KOLTE, *Modern Casting* (1985) 33.
107. D. ARGO and J. E. GRUZLESKI, in Proceedings of International Symposium on Reduction and Casting of Aluminium, Montreal, Canada, August 1988 (Pergamon, New York, 1988) p. 263.
108. J. E. GRUZLESKI, N. HANDIAK, H. CAMPBELL and B. CLOSSET, *AFS Trans.* **94** (1986) 167.
109. B. CLOSSET and J. E. GRUZLESKI, in Proceedings of 56th World Foundry Congress, Düsseldorf, May 1989, paper no. 32 (1989).
110. M. D. HANNA, S. LU and A. HELLAWELL, *Met. Trans. A* **15A** (1986) 459.
111. S. C. FLOOD and J. D. HUNT, *Met. Sci.* **15** (1981) 287.
112. G. K. SIGWORTH, S. SHIVKUMAR and D. APELIAN, *AFS Trans.* **97** (1989) 811.
113. H. IWAHORI, K. YONEKURA, Y. YAMAMOTO and M. NAKAMURA, *ibid.,* **98** (1990) 167.
114. *Idem., Imono* **61** (1989) 31.
115. Y. W. LEE, E. CHANG and C. F. CHIEU, *Met. Trans. B* **21B** (1990) 715.
116. W. MICHELS and S. ENGLER, *Giessereiforschung* **41** (1989) 174.
117. B. L. TUTTLE, A. KESLINKE, D. TWAROG and E. DANIELS, *AFS Trans.* **97** (1989) 889.
118. M. GARAT, "Hypo-Eutectic Al–Si Alloys, Control of the Eutectic Structures" (Aluminium Pechiney, Pechiney, 1980).
119. F. L. ARNOLD and J. S. PRESTLEY, *AFS Trans.* **69** (1961) 129.
120. A. J. CLEGG and A. A. DAS, *Br. Foundryman* **70** (1977) 56.
121. J. CHARBONNIER, *AFS Trans.* **92** (1984) 907.
122. B. E. CARLSON and R. D. PEHLKE, *ibid.* **97,** (1989) 903.
123. J. H. O'DETTE, *Trans. AIME* **208** (1957) 924.
124. A. N. TURNER and A. J. BRYANT, *J. Inst. Met.* **95** (1967) 353.
125. O. KUBASCHEWSKI, *et al.,* "Gases and Metals" (Iliffe, London, 1970).
126. D. STEIN, *AFS Trans.* **88** (1980) 631.
127. G. K. SIGWORTH, *ibid.* **95** (1987) 73.
128. J. C. JAQUET and H. J. HUBER, *Geissereiforschung* **38** (1986) 11.
129. M. TSUKUDA, T. SUZUKI, I. FUKUI and M. HARADA, *J. Jpn. Inst. Met.* **29** (1979) 437.
130. C. VASS, in Proceedings of Conference on International Molten Metal Processing, American Foundrymen's Society, Des Plaines, Illinois (1986) p. 101.
131. U. HONMA and S. KITAOKA, *Aluminium* **60** (1984) E780.
132. G. K. SIGWORTH, in Proceedings of Conference on International Molten Metal Processing, American Foundrymen's Society, Des Plaines, Illinois (1986) p. 75.
133. A. SAIGAL, *AFS Trans.* **94** (1986) 219.
134. S. SHIVAKUMAR, S. RICCI Jr, B. STEENHOFF, D. APELIAN and G. SIGWORTH, *ibid.* **97** (1989) 791.
135. N. FAT-HALLA, in Proceedings of Conference, "Current Advances in Mechanical Properties and Production III", Cairo University, Cairo, Egypt, December 1985 (1985) p. 28.
136. G. K. SIGWORTH, *AFS Trans.* **91** (1983) 7.
137. N. L. KUTSENOK, I. N. GANIEV and V. N. YANCHUK, *Metallovedemie i Termicheskaya Obrabotka Metallov* No. 2, (February 1987) 45.
138. P. REZNICEK and M. HOLMANOVA, *Slevárenstvi* **34** (1986) 108.
139. TRAENKNER, *Modern Casting* (October 1982) pp. 36–37.
140. J. A. EADY and D. M. SMITH, *Mater. Forum* **9** (1986) 217.
141. I. MIKI and T. KIDO, *Die-Cast Eng.* (April 1974) 22.
142. T. E. GEBHARD Jr, *Cast. Eng.* (Spring 1976) 16.
143. G. M. GLENN, *SAMPE Quart.* (1976) 1.
144. S. N. TIWARI, A. K. GUPTA and S. L. MALHOTRA, *Br. Foundryman* **79** (1986) 129.
145. E. SCHEUER, *J. Inst. Met.* **85** (1956–57) 521.
146. V. K. AFANAS'EV and A. N. PRUDNIKOV, *Liteinoe Proivodstvo* No. 9 (1988) 12.
147. W. R. OPIE and N. J. GRANT, *Foundry* **78** (1950) 104.
148. R. W. RUDDLE and A. CIBULA, (Institute of Metals, London, 1965).
149. R. K. OWENS, *et al., AFS Trans.* **65** (1957) 424.
150. R. JAY and A. CIBULA, *Foundry Trade J.* **101** (1956) 131, 407.
151. M. K. SURAPPA, E. BLANK and J. C. JAQUET, *Scripta Metall.* **20** (1986) 1281.
152. C. W. BOOTH and A. J. CLEGG, *Br. Foundryman* **77** (1984) 96.
153. A. G. SZEKELY, in Proceedings of 2nd International Aluminium Extrusion Technology Seminar, Vol. 1 (1977) p. 35.
154. M. V. BRANT, D. C. BONE and E. F. EMLEY, *Met. Soc. AIME,* TMS Paper No. A70–51 (1970).
155. G. W. M. van WIJK and D. M. ACKERMANN, *Light Metals* **2** (1978) 235.
156. G. K. SIGWORTH, *Modern Casting* (March 1988) (1988) 42.
157. D. W. PATTLE, *Foundryman* **81** (1988) 232.
158. O. G. GJOSTEEN *et al.* TMS Paper No. 71–39 (1971).
159. C. S. SIVARAMAKRISHNAN and R. K. MAHANTI, *NML Tech. J.* **26** (1984) 5.
160. W. SCHAEFERS, J. G. KRUGER and T. STEINHAUSER, *Giesserei* **73** (1986) 432.
161. A. CHOUDHURY and M. LORKE, *Aluminium* **65** (1989) 462.
162. S. L. ARCHBUTT, *J. Inst. Met.* **227** (1925) 33.
163. P. M. HULME, *Steel* **119** (15) (1946) 108.
164. *Idem, ibid.* **119** (16) (1946) 110.
165. B. A. BAUM, K. T. KUROCHKIN and P. V. UMRIKHIN, *Izvest. Vuz-Chern. Met.* (1961) 22.
166. W. GELLER, *Z. Metallkde* **35** (1943) 213.
167. R. D. PEHLKE and A. L. BEMENT Jr, *Trans. Met. Soc. AIME* (1962) 1237.
168. J. BOTOR, *Prace Inst. Met. Niezel.* **7** (1978) 1.
169. *Idem, Aluminium* **56** (1980) 519.

170. G. K. SIGWORTH and T. A. ENGH, *Met. Trans. B.* **13B** (1982) 447.
171. *Idem, Scand. J. Metall.* **11** (1982) 143.
172. T. A. ENGH and T. PEDERSEN, *Light Metals* (1984) 1329.
173. R. J. ADAMO and C. L. BROOKS, *Met. Soc. AIME*, TMS Paper No. 72–80 (1972).
174. A. KAYE, *Foundry Trade J.* **164** (1983) 3261.
175. A. L. ZOLOTOI, K. N. MILITSYN and O. P. NAUMKIN, *Sov. Cast Technol.* **5** (1988) 55.
176. J. E. DORE, J. C. YARWOOD and J. A. FORD, *Light Metals, AIME* **2** (1976) 567.
177. H. O. TITZE, *ibid.* **2** (1973) 451.
178. G. D. DENYER, *Rev. Metallurgie* **59** (1962) 857.
179. J. E. DORE, P. E. SEVIER and J. C. YARWOOD, US Patent No. 3 854 934 (1974).
180. F. R. MOLLARD and N. DAVIDSON, *AFS Trans.* **86** (1978) 501.
181. A. G. SZEKELY, US Patent 3 227 547 (1966).
182. M. J. BRUNO, N. JARRETT, B. L. SLAUGENHAUPT and R. E. GRAZIANO, US Patent 3 839 019 (1974).
183. M. GARAT, *Hommes et Fonderie* (December 1989) 17.
184. A. R. ANDERSON, *AFS Trans.* **95** (1987) 533.
185. J. M. FUQUA, *ibid.* **95** (1987) 635.
186. R. J. HARRISS, *Foundry Trade J.* (10 March 1989) 148.
187. J. T. BOPP, D. V. NEFF and E. P. STANKIEWICZ, *Light Metals* (1987) 729.
188. S. KASTNER and J. KRUGER, *Aluminium*, **58** (1982) E52.
189. YAZANA *et al.* in Proceedings of 4th International Conference on Vacuum Metallurgy, Tokyo, 1973 (1973) p. 86.
190. G. S. MAKAROV *et al.*, "Legirovonie i Obrabolka Legkikh Splavov" (Alloy and Treatment of Light Alloys) (Nauk, Moscow, 1981) p. 66 (in Russian).
191. W. HILGENFELDT and I. HILPMANN, *Giessereitechnik* **28** (1982) 40.
192. T. CURAVIC, "Giesserei Fachtagung", Portoz, Jugoslavia (1983).
193. "Vakuum-Entgasungsanlagen für Aluminium and Aluminium legierungen" (Leybold AG, Hanau, 1984).

Received 2 September 1991
and accepted 17 January 1992